Title**:**

Group I p21-activated kinases (PAKs) are largely dispensable for insulin-stimulated glucose uptake in mouse skeletal muscle

Lisbeth L. V. Møller[1], Merna Jaurji[1], Rasmus Kjøbsted[1], Giselle A. Joseph[2], Agnete B. Madsen[1], Jonas R. Knudsen[1], Annemarie Lundsgaard[1], Nicoline R. Andersen[1], Peter Schjerling[3,4], Thomas E. Jensen[1], Robert S. Krauss[2], Erik A. Richter[1*], and Lykke Sylow[1*]

[1] Section of Molecular Physiology, Department of Nutrition, Exercise and Sports, Faculty of Science, University of Copenhagen, Denmark

[2] Department of Cell, Developmental, and Regenerative Biology, Icahn School of Medicine at Mount Sinai, New York, NY 10029 USA

[3] Institute of Sports Medicine, Department of Orthopedic Surgery M, Bispebjerg Hospital, Denmark

[4] Center for Healthy Aging, Faculty of Health Sciences, University of Copenhagen, Denmark

[*]*Corresponding authors and persons to who reprint requests should be addressed. Authors contributed equally.*

Lykke Sylow, Lshansen@nexs.ku.dk, phone +4520955250

Erik Arne Richter, Erichter@nexs.ku.dk, phone +4528751626

Universitetsparken 13, 2100 Copenhagen Oe, Denmark

Short title: Group I PAKs and insulin-stimulated skeletal muscle glucose uptake

Number of figures: 7 (+ 6 supplemental figures)

Non-standard abbreviations

2DG: 2-Deoxyglucose

AUC: Area under the curve

BCA: Bicinchoninic acid

BW: Body weight

dKO: Double knockout

EDL: Extensor digitorum longus

FM: Fat mass

GLUT4: Glucose transporter 4

GTT: Glucose tolerance test

HFD: High-fat diet

HOMA-IR: Homeostatic Model Assessment of Insulin Resistance

ITT: Insulin tolerance test

i.p.: Intraperitoneal

KO: Knockout

L6-GLUT4myc: Rat L6 skeletal muscle cells overexpressing myc-tagged GLUT4

LBM: Lean body mass

mKO: Muscle-specific knockout

NOX: NADPH oxidase

PAK: p21-activated kinase

PI3K: Phosphoinositide 3-kinase

RER: Respiratory exchange ratio

r.o.: Retro-orbital

VO_2: Oxygen uptake

Abstract

Glucose transport into skeletal muscle is essential for maintaining whole-body glucose homeostasis and accounts for the majority of glucose disposal in response to insulin. The group I p21-activated kinase (PAK) isoforms PAK1 and PAK2 have been shown to be activated in response to insulin in skeletal muscle. Moreover, PAK1/2 signalling is impaired in insulin-resistant mouse and human skeletal muscle and PAK1 has been suggested to be required for insulin-stimulated GLUT4 translocation. However, the relative contribution of PAK1 and PAK2 to insulin-stimulated glucose uptake in mature skeletal muscle is unresolved. The aim of the present investigation was to determine the requirement for PAK1 and PAK2 in whole-body glucose homeostasis and insulin-stimulated glucose uptake in skeletal muscle. Glucose uptake was measured in isolated skeletal muscle incubated with a pharmacological inhibitor (IPA-3) of group I PAKs and in muscle from whole-body PAK1 knockout (KO), muscle-specific PAK2 (m)KO and double whole-body PAK1 and muscle-specific PAK2 knockout mice. The whole-body respiratory exchange ratio, indicative of substrate utilization, was largely unaffected by lack of PAK1 and/or PAK2. Whole-body glucose tolerance was mildly impaired in PAK2 mKO, but not PAK1 KO mice. In contrast to a previous study of GLUT4 translocation in PAK1 KO mice, PAK1 KO muscles displayed normal insulin-stimulated glucose uptake *in vivo* and in isolated muscle. On the contrary, glucose uptake was slightly reduced (-12-18%) in response to insulin in glycolytic extensor digitorum longus muscle lacking PAK2. In conclusion, group I PAKs are largely dispensable for the regulation of whole-body glucose homeostasis and skeletal muscle glucose uptake. Thus, the present study challenges that group I PAKs, and especially PAK1, are necessary regulators of insulin-stimulated glucose uptake in skeletal muscle.

Introduction

The skeletal muscles act as a major glucose sink for disposal of glucose from the blood and are therefore essential in maintaining whole-body glucose homeostasis. It is important to understand the mechanisms regulating glucose uptake by skeletal muscle, in part because skeletal muscles account for the majority of insulin-mediated whole-body glucose disposal [1,2] and muscle insulin resistance is an early defect in the pathophysiology of peripheral insulin resistance and type 2 diabetes mellitus [1,3].

Insulin stimulates glucose uptake in skeletal muscle by activation of a signalling cascade that leads to the translocation of glucose transporter (GLUT)4-containing vesicles to the sarcolemma and transverse tubuli [4]. This signalling cascade has been proposed to include activation of p21-activated kinase 1 (PAK1) downstream of PI3K [5–7]. PAKs are serine/threonine kinases and PAK1, PAK2 and PAK3 constitute the group I PAKs. Group I PAKs have been extensively studied as part of numerous signalling networks that regulate essential cellular activities, including cell proliferation, differentiation, apoptosis, and cytoskeleton dynamics [8,9]. PAKs are downstream targets of the Rho GTPases Cdc42 and Rac1 [10]. Previous studies suggest that only PAK1 and PAK2 are expressed in skeletal muscle, whereas PAK3 mRNA and protein expression is below the detection limit [6,8,11]. In muscle cells and mouse skeletal muscle, PAK1 is proposed to be required for GLUT4 translocation in response to insulin stimulation [6,7], likely downstream of Rac1 [12–17]. Thus, together with Akt, proposed to regulate GLUT4 translocation via phosphorylation of the Rab GTPase-activating protein TBC1D4 [18–20], Rac1-PAK1 activation is suggested to be necessary for insulin-stimulated GLUT4 translocation.

Upon activation of PAK1 and PAK2, conformational changes allow autophosphorylation of T423 and T402, respectively, thereby relieving the autoinhibition of PAK1 and PAK2 [10,21,22]. In

vastus lateralis muscle from subjects with obesity and type 2 diabetes, phosphorylation of PAK1/2 at T423/402 in response to insulin was 50% reduced compared to healthy controls [15]. Likewise, insulin-stimulated pPAK1/2 T423/402 was diminished in palmitate-treated insulin-resistant L6 myotubes, even though upstream of PAK1/2, insulin-stimulated Rac1-GTP binding (i.e. activation) was not impaired [23]. Together, these studies [15,23] associate dysregulated activity of PAK1 and PAK2 with insulin resistance. In addition, a pharmacological inhibitor of group I PAKs, IPA-3 abolished insulin-stimulated GLUT4 translocation and glucose uptake into L6 myoblasts and myotubes, respectively, overexpressing myc-tagged GLUT4 (L6-GLUT4myc) [6]. This indicates that group I PAKs are required for insulin-stimulated glucose uptake. This effect has largely been ascribed to PAK1, as whole-body genetic ablation of PAK1 in mice impaired glucose tolerance [7,24] and blocked insulin-stimulated GLUT4 translocation in skeletal muscle [7]. Further supporting PAK1 being the major PAK isoform regulating GLUT4 translocation, insulin-stimulated GLUT4 translocation was unaffected by a 75% knockdown of PAK2 in L6-GLUT4myc myoblasts [6]. The suggested downstream mechanisms whereby PAK1 regulates GLUT4 translocation include simultaneous cofilin-mediated actin depolymerization and N-WASP-cortactin-mediated actin polymerization [6,25,26].

Although such studies implicate group I PAKs, and in particular PAK1, in the regulation of glucose homeostasis and GLUT4 translocation in skeletal muscle, the relative role of PAK1 and PAK2 in insulin-stimulated glucose uptake remains to be identified in mature skeletal muscle. Therefore, we performed a systematic series of pharmacologic and genetic experiments to analyze the involvement of group I PAKs in the regulation of insulin-stimulated glucose uptake in mouse skeletal muscle. We hypothesized that group I PAKs, and in particular PAK1, would be necessary for glucose uptake in response to insulin. Contradicting our hypothesis, our results revealed that group I PAKs are largely dispensable for insulin-stimulated glucose uptake in skeletal muscle.

Results

Pharmacological inhibition of group I PAKs partially reduces insulin-stimulated glucose uptake in mouse soleus muscle. To investigate the involvement of group I PAKs in insulin-stimulated glucose uptake in mouse skeletal muscle, we first analyzed 2DG uptake in isolated soleus and extensor digitorum longus (EDL) muscle in the presence of a pharmacological inhibitor, IPA-3. While glucose uptake *in vivo* is influenced by glucose delivery, GLUT4 translocation and muscle metabolism [27], glucose delivery is constant in isolated skeletal muscle and surface membrane GLUT4 is the limiting factor [28–30]. Therefore, 2-Deoxyglucose (2DG) uptake in isolated muscles likely reflects GLUT4 translocation. IPA-3 is a well-characterized inhibitor of group I PAKs (PAK1-3) [6,31] and shown to completely abolish insulin-stimulated GLUT4 translocation and glucose uptake in L6-GLUT4myc myoblasts and myotubes, respectively [6]. In soleus, 2DG uptake increased 4.5-fold upon maximal insulin-stimulation, an increase that was partly reduced (-20%) in IPA-3-treated muscles (Fig. 1A). IPA-3 did not significantly (p=0.080) impair insulin-stimulated (+2.4-fold) 2DG uptake in EDL muscle (Fig. 1B). We confirmed that IPA-3 treatment abolished insulin-stimulated phosphorylation of (p)PAK1 T423 in both soleus and EDL muscle (Fig. 1C+D). In contrast, insulin-stimulated pAkt T308 (Fig. 1E+F) and pAkt S473 (Fig. 1G+H) were unaffected by IPA-3 treatment, suggesting that IPA-3 did not interfere with insulin signalling to Akt. Altogether this suggests that group I PAKs are only partially involved in insulin-stimulated glucose uptake in isolated mouse muscle.

PAK1 knockout does not affect whole-body glucose tolerance or insulin-stimulated glucose uptake in isolated skeletal muscle. We next sought to confirm our findings in mice with whole-body lack of the PAK1 isoform (PAK1 KO) and therefore a complete knockout of PAK1 in skeletal muscle (Fig.

2A). In chow-fed mice, fat mass, lean body mass, body weight and energy intake (Fig. 2B-C) were similar between whole-body PAK1 KO and littermate controls, as also reported previously [33]. During a glucose tolerance test (GTT), the lack of PAK1 had no effect on the blood glucose response (Fig. 2D-E) or plasma insulin concentration (Fig. 2F). Additionally, Homeostatic Model Assessment of Insulin Resistance (HOMA-IR), a measure of basal glucose homeostasis (Fig. 2G), and both submaximal and maximal insulin-stimulated 2DG uptake in isolated soleus and EDL muscle were unaffected by PAK1 KO (Fig. 2H-I). Thus, unexpectedly, genetic ablation of PAK1 alone did not impair whole-body glucose tolerance, or skeletal muscle insulin sensitivity (submaximal insulin-stimulated glucose uptake) or insulin responsiveness (maximal insulin-stimulated glucose uptake) in divergence to previous reports [6,7,9].

PAK1 is not required for insulin-stimulated glucose uptake in lean or diet-induced insulin-resistant mice in vivo. Our findings on insulin-stimulated glucose uptake in isolated muscle from chow-fed PAK1 KO mice conflicted with a previous study reporting impaired glucose tolerance in PAK1 KO mice and defects in insulin-stimulated GLUT4 translocation in skeletal muscle *in vivo* [7]. Therefore, we further explored the effect of PAK1 KO on insulin-stimulated glucose uptake in skeletal muscle *in vivo*. Additionally, we fed a subgroup of PAK1 KO and control littermate mice a 60E% high-fat diet (HFD) for 21 weeks to investigate the role of PAK1 in insulin-resistant muscle. Insulin administration lowered blood glucose by 5.4±0.5 mM (-47%) in chow-fed control mice (Fig. 3A). In HFD-fed control mice, blood glucose dropped 3.0±0.9 mM (-26%) upon insulin administration (Fig. 3B). Lack of PAK1 had no impact on either basal blood glucose or whole-body insulin tolerance on either of the diets (Fig. 3A-B). Insulin increased glucose uptake in muscles from chow-fed (Gastrocnemius: 8.1-fold; Quadriceps: 8.5-fold, Triceps brachii: 12.3-fold; Soleus: 8.9-fold) and HFD-fed (Gastrocnemius: 3.5-fold; Quadriceps: 1.8-fold, Triceps brachii: 4.3-fold; Soleus: 11.6-fold) control mice (Fig. 3C-D). Consistent with our findings in isolated muscle, we

observed no effect of PAK1 KO on basal or insulin-stimulated glucose uptake *in vivo* in muscle of either chow-fed mice or in insulin-resistant muscles from HFD-fed mice. Like glucose uptake, 2DG clearance from the plasma was unaffected by PAK1 KO in all of the investigated muscles (Fig. S1A-B). Importantly, circulating [^{3}H]-2DG availability was unaffected by genotype on both of the diets (Fig. S1C). As in chow-fed mice, lack of PAK1 in HFD-fed mice had no effect on fat mass, lean body mass, body weight or energy intake (Fig. S1D-E). Similarly, whole-body glucose tolerance (Fig. S1F-G), plasma insulin concentration during the GTT (Fig. S1H) and HOMA-IR (Fig. S1I) were unaffected by PAK1 KO in HFD-fed mice. Thus, PAK1 is dispensable for *in vivo* insulin-stimulated muscle glucose uptake in both the healthy lean and the diet-induced insulin-resistant state.

Whole-body substrate utilization is unaffected by genetic ablation of PAK1 and PAK2. Because of discrepancies in the data resulting from the use of a global pharmacological inhibitor of group I PAKs and data resulting from PAK1 KO mice, we next sought to determine the relative contribution and involvement of PAK1 and PAK2 in insulin signalling and glucose uptake in skeletal muscle. Double knockout mice with whole-body knockout of PAK1 and muscle-specific knockout of PAK2 (1/m2 dKO) were generated as previously described [8]. By crossing 1/m2 dKO mice with littermate controls, a cohort was generated consisting of whole-body PAK1 KO, muscle-specific PAK2 (m)KO, 1/m2 dKO and littermate control mice. While no band for PAK1 could be detected in muscles lacking PAK1, muscles lacking PAK2 displayed only a partial reduction in band intensity in the immunoblots for PAK2 (Fig. 4A). This is likely due to the fact that PAK1 KO mice are whole-body knockouts, while PAK2 mKO mice are muscle-specific and other cell types within skeletal muscle tissue could thus contribute to the signal obtained in the PAK2 immunoblots. In a previous study, PAK3 was not detectable at the protein level in 1/m2 dKO muscle [8].

As previously shown [8,34], 1/m2 dKO mice weighed less (-12%) than control littermates (Fig. 4B, Fig. S2A-B) due to reduced (-12%) lean body mass (Fig. 4C, Fig. S2C-D). Body weight and lean body mass decreased to the same extent in 1/m2 dKO mice, leaving lean body mass percentage largely unaffected (Fig. S2E-G). Using calorimetric chambers, we monitored whole-body metabolism for 72 hours during the light and dark period. On day 2, the mice fasted during the dark period followed by refeeding on day 3. Oxygen uptake (VO_2; Fig. 4D, Fig. S3A-B) and respiratory exchange ratio indicative of substrate utilization (RER; Fig. 4E, Fig. S3C-D) were largely unaffected by genotype with only a slightly higher RER in mice lacking PAK2 (PAK2 mKO and 1/m2 dKO mice) upon fasting. Similar substrate utilization was obtained despite reduced habitual activity in the dark period in mice lacking PAK2, an effect largely driven by a decreased activity in d1/2KO mice and an increased activity in male PAK1 KO mice (Fig. 4F; Fig. S3E-F). Supporting the lower activity levels, energy intake was decreased (-11%) in 1/m2 dKO mice compared to PAK1 KO mice on day 1 (Fig. S3G) due to lower energy intake in the dark period (Fig. 4G). Upon refeeding, energy intake was reduced in mice lacking PAK2 (Fig. 4G; Fig. S3G) driven by a lower energy intake in the dark period in female mice lacking PAK2 (Fig. S3H-K). Altogether, these data suggest that lack of PAK1 and/or PAK2 are not compromising metabolic regulation during the light/dark period or in response to fasting/refeeding.

Glucose tolerance is slightly reduced in mice lacking PAK2 in skeletal muscle. To test dependency on PAK1 and/or PAK2 in glucose handling and insulin sensitivity, we next investigated glucose and insulin tolerance in the 1/m2 dKO mouse strain. Blood glucose concentration in the fed state was similar between the genotypes (Fig. 5A, Fig. S4A-B). The blood glucose response to a glucose load was slightly increased in mice lacking PAK2 in skeletal muscle as evident by the increased area under the blood glucose curve (Fig. 5B-C). This was primarily driven by impaired glucose tolerance in female PAK2 mKO mice (Fig. S4C-F). Plasma insulin concentration during the GTT was

unaffected by lack of PAK1 (Fig. 5D) In contrast, plasma insulin in male PAK2 mKO mice was slightly elevated compared to 1/m2 dKO mice and tended (p=0.055) to be higher than control littermates (Fig. S4G-H). This indicates impaired insulin sensitivity in male PAK2 mKO mice, but HOMA-IR was unaffected by lack of PAK1 and/or PAK2 (Fig. 5E, Fig. S5A-B). In addition, even though fasted blood glucose immediately before an insulin tolerance test (ITT) was modestly reduced in PAK2 mKO mice (Fig. S5C-E), the blood glucose response to an ITT was largely unaffected by lack of either PAK1 and/or PAK2 (Fig. 5F, Fig. S5F-G). Thus, despite slightly impaired glucose tolerance in mice lacking PAK2 in skeletal muscle, neither adverse effects on plasma insulin nor defects in insulin sensitivity could be detected.

Insulin-stimulated glucose uptake relies partially on PAK2 in EDL, but not soleus muscle, while PAK1 is not involved. To determine the relative contribution and involvement of PAK1 and PAK2 in glucose uptake in skeletal muscle, we next investigated insulin-stimulated 2DG uptake in isolated soleus and EDL. To our surprise, soleus muscle lacking PAK1 and PAK2 displayed normal insulin-stimulated 2DG uptake compared to control littermates (Fig. 6A,C). In contrast, lack of PAK2 in EDL muscle caused a modest reduction (PAK2 mKO: -18%; d1/2KO: -12%) in insulin-stimulated 2DG uptake (Fig. 6B,D). Thus, in oxidative soleus muscle, group I PAKs are dispensable for normal insulin-stimulated glucose uptake, whereas in glycolytic EDL muscle PAK2 plays a minor role.

PAK2 regulates TBC1D4 protein expression and signalling. Lastly, we looked into the effects of PAK1 and PAK2 on insulin-stimulated signalling. All groups displayed normal basal and insulin-stimulated pAkt S473 (Fig. 7A-B, Fig. S6A-B) and pAkt T308 (Fig. 7C-D, Fig. S6C-D) and Akt2 protein expression (Fig. S6E-F) compared to control littermates in both soleus and EDL muscle. In contrast, lack of PAK2 increased protein expression of Akt's downstream target, TBC1D4 in soleus muscle (PAK2 mKO: +47%; d1/2KO: +20%) (Fig. 7E), while reducing TBC1D4 expression in

EDL (PAK2 mKO: -33%; d1/2KO: -9%) (Fig. 7F). In soleus, basal and insulin-stimulated pTBC1D4 T642 was similar in all groups (Fig. 7G, Fig. S6G), suggesting that even with increased TBC1D4 expression, signalling through this pathway was normal. Concomitant with the decreased TBC1D4 expression in EDL muscle, lack of PAK2 reduced insulin-stimulated pTBC1D4 T642 (Fig. 7H, Fig. S6H) driven by attenuated (-46%) insulin-stimulated pTBC1D4 T642 in PAK2 mKO mice compared to control littermates (Fig. S6H). Knockout of TBC1D4 has been associated with lower GLUT4 protein abundance in some muscles [35,36]. Whereas GLUT4 protein expression was normal in soleus (Fig. 7I), GLUT4 protein expression was mildly reduced in EDL in PAK2 mKO mice compared to littermate control (Fig. 7J). Thus, the slightly reduced insulin-stimulated glucose uptake in EDL muscle lacking PAK2 was concomitant with downregulated TBC1D4 signalling and GLUT4 expression supporting a role for PAK2, but not PAK1, in insulin-stimulated glucose uptake.

Discussion

We here undertook a systematic investigation into the requirement of the group I PAK isoforms in muscle glucose uptake and whole-body metabolic regulation. In contrast to previous literature, our results show that PAK1 is dispensable for insulin-stimulated glucose uptake in skeletal muscle, while PAK2 may play a minor role. Using a cohort of whole-body PAK1 KO mice and another cohort of transgenic mice lacking either PAK1 (whole-body), PAK2 (muscle-specific), or jointly lacking both PAK1 and muscle PAK2, we show that PAK1 is not required in insulin-stimulated muscle glucose uptake *in vivo* or in isolated muscles. In accordance, we found no effect of whole-body PAK1 KO on glucose tolerance in either mice fed a standard chow diet (insulin sensitive mice) or in mice fed a HFD (insulin-resistant mice). In contrast, PAK2 seemed partially involved in

insulin-stimulated glucose uptake in EDL muscle. This could potentially explain the slightly impaired glucose tolerance with the muscle-specific knockout of PAK2 in mice. Nevertheless, supporting only a minor role for skeletal muscle PAK2 in the whole-body substrate utilization, RER was largely unaffected by lack of PAK1 and/or PAK2 and only slightly elevated in mice lacking PAK2 when challenged by fasting.

In a previous study, the increase in GLUT4 abundance at the plasma membrane in response to insulin measured was completely abrogated in PAK1 KO muscle as measured by subcellular fractionation of homogenates of hindlimb skeletal muscles [7], suggesting that PAK1 is necessary for insulin-stimulated GLUT4 translocation. Although glucose uptake was not assessed in that study [7], this indicated a key role for PAK1 in regulating glucose uptake in mouse skeletal muscle. Surprisingly, PAK1 was not required for insulin-stimulated glucose uptake in our hands. Furthermore, in our study, both chow- and HFD-fed PAK1 KO mice displayed blood glucose concentrations similar to control littermates during a GTT. This was in contrast to previous studies reporting impaired glucose tolerance in chow-fed PAK1 KO mice [7,24] and elevated fasting blood glucose in PAK1 KO mice fed a western diet (45E% fat) [33]. Instead, despite the previous finding that insulin-stimulated GLUT4 translocation was unaffected by a 75% knockdown of PAK2 in L6-GLUT4myc myoblasts [6], we found that muscle-specific PAK2 KO slightly impaired glucose tolerance and insulin-stimulated glucose in mouse skeletal muscle. These discrepancies between our and previous findings are difficult to delineate but might be due to methodological differences. Wang et al. [7] used a crude fractionation method to measure GLUT4 translocation, whereas we analyzed the direct outcome hereof: glucose uptake. Although the insulin-induced increase in 3-O-methylglucose transport correlates with the increase in cell surface GLUT4 protein content in human skeletal muscle strips [40], discrepancies between the presence of GLUT4 at the plasma membrane and glucose uptake have occasionally been reported in cell culture studies [37–39].

Another potential explanatory factor could be that our studies were conducted in both female and male mice, whereas past studies in PAK1 KO mice have been conducted in 4-6 months old male mice [7,33]. However, our data suggest no major differences between female and male mice in the response to lack of PAK1 and/or PAK2 on the whole-body metabolic parameters measured. Instead, the discrepancies between our and previous findings could be due to an effect of age, as our studies were conducted in mice at different ranges of age (10-37 of weeks age at the terminal experiment). In fact, age-dependent myopathy and development of megaconial mitochondria have been reported in the 1/m2 dKO mice [34]. Regardless, even though a role for group I PAKs in age-related insulin resistance should be further investigated, our investigation suggests that group I PAKs are dispensable in regulating whole-body glucose homeostasis or insulin-stimulated glucose uptake in skeletal muscle.

In the current study, pharmacological inhibition of group I PAKs inhibited muscle glucose uptake in response to insulin. Similarly, IPA-3 previously inhibited insulin-stimulated GLUT4 translocation and glucose uptake in L6-GLUT4myc myoblasts and myotubes, respectively [6]. IPA-3 is a non-ATP-competitive allosteric inhibitor of all group I PAKs (PAK1, 2, and 3). IPA-3 binds covalently to the regulatory CRIB domain of group I PAKs, thereby preventing binding to PAK activators, such as Rac1 [31]. Although IPA-3 is reported to be a highly selective and well-described inhibitor of group I PAKs that does not affect other groups of PAKs or similar kinases tested [31], pharmacological inhibitors often have off-target effects [32] which is a concern. It is also possible that acute IPA-3-induced inhibition of group I PAKs elicits more potent effects compared with jointly knockout of PAK1 and PAK2 because the transgenic manipulations have been present from birth and may thus have resulted in compensatory changes. The development of inducible muscle-specific group I PAK deficient models could help clarify this. Importantly, any possible compensatory mechanisms cannot be via redundancy with group I PAKs, as PAK1 and PAK2 are

306 removed genetically, and even in 1/m2 dKO mice, PAK3 cannot be detected at the protein level [8].
307 This emphasizes that group I PAKs are largely dispensable for insulin-stimulated glucose uptake in
308 skeletal muscle.

309 Our hypothesis was that group I PAKs would be significantly involved in insulin-stimulated
310 glucose uptake because of the established necessity of their upstream activator, Rac1 [12–17]. Our
311 findings suggest that Rac1 does not exclusively mediate insulin-stimulated glucose uptake through
312 group I PAKs. Another downstream target of Rac1 is RalA. GLUT4 translocation induced by a
313 constitutively activated Rac1 mutant was abrogated in L6-GLUT4myc myoblasts upon RalA
314 knockdown [41] and, importantly, overexpression of a dominant-negative mutant of RalA reduced
315 GLUT4 translocation in response to insulin in mouse gastrocnemius muscle fibres [42].
316 Additionally, Rac1 is an essential component in the activation of the NADPH oxidase (NOX)
317 complex [43,44]. In L6-GLUT4myc myotubes, reactive oxygen species have been reported to
318 induce NOX2-dependent GLUT4 translocation in response to insulin [45]. Insulin-stimulated
319 NOX2 regulation in mature muscle remains to be investigated. However, a recent study suggested a
320 role for Rac1 in the regulation of muscle glucose uptake through activation of the NOX2 in
321 response to exercise [46]. Since Rac1 is required for both contraction- and insulin-stimulated
322 glucose uptake in isolated mouse muscle [15,47], Rac1 could also be involved in insulin-stimulated
323 glucose uptake via NOX2 activation. Consequently, future studies should aim to investigate other
324 players downstream of Rac1 since group I PAKs seem to be largely dispensable for glucose uptake
325 in mature skeletal muscle.

326 Based on our present findings, we conclude that even though PAK2 may be a minor requirement for
327 insulin-stimulated glucose uptake in EDL muscle, group I PAKs are largely dispensable in the
328 regulation of whole-body glucose homeostasis and insulin-stimulated glucose uptake in mouse
329 skeletal muscle.

330

331 **Materials and Methods**

332 ***Animal experiments.*** Female C57BL/6J mice (Taconic, Denmark) were used for all inhibitor
333 incubation studies. Mice received standard rodent chow diet (Altromin no. 1324; Brogaarden,
334 Denmark) and water ad libitum.

335 *Whole-body PAK1$^{-/-}$ mice*. Whole-body PAK1$^{-/-}$ mice on a C57BL/6J background were generated as
336 previously described [48]. The mice were obtained by heterozygous crossing. PAK1$^{-/-}$ mice
337 (referred to as PAK1 KO) and paired littermate PAK1$^{+/+}$ mice (referred to as controls) were used for
338 experiments. Female and male mice were used for measurements of body composition, glucose
339 tolerance and insulin-stimulated glucose uptake in isolated muscle. The mice were 12-24 weeks of
340 age at the time of tissue dissection and measurement of glucose uptake. Number of mice in each
341 group: Control, *n = 6/7* (female/male); PAK1 KO, *n = 4/8*. Mice received standard rodent chow
342 diet and water ad libitum.

343 For measurement of *in vivo* insulin-stimulated glucose uptake in chow- and 60E% HFD (no.
344 D12492; Brogaarden, Denmark)-fed PAK1 KO mice, mice were assigned to a chow or HFD group.
345 Chow-fed mice were 10-24 weeks of age at the time of glucose uptake measurements and tissue
346 dissection. Number of mice in each group: Control-Chow, *n = 14/8* (female/male); PAK1 KO-
347 Chow, *n = 6/4*. For mice receiving HFD, the diet intervention started at 6-16 weeks of age and
348 lasted for 21 weeks. HFD-fed mice were used for body composition, glucose tolerance and *in vivo*
349 glucose uptake and were 27-37 weeks of age at the time of glucose uptake measurements and tissue
350 dissection. Number of mice in each group: Control-HFD, *n = 7/7* (female/male); PAK1 KO-HFD, *n*
351 *= 11/5*. Energy intake was measured over a period of 10 weeks in another cohort of mice. Number

of mice in each group: Chow, *n = 8/8* (Control/PAK1 KO); HFD, *n = 8/8*. Mice had access to their respective diet and water ad libitum.

Double PAK1$^{-/-}$;PAK2$^{fl/fl}$;MyoD$^{iCre/+}$ mice. Double knockout mice with whole-body knockout of PAK1 and conditional, muscle-specific knockout of PAK2, PAK1$^{-/-}$;PAK2$^{fl/fl}$;MyoD$^{iCre/+}$ were generated as previously described [8]. The mice were on a mixed C57BL/6/FVB background. PAK1$^{-/-}$;PAK2$^{fl/fl}$;MyoD$^{iCre/+}$ were crossed with PAK1$^{+/-}$;PAK2$^{fl/fl}$;MyoD$^{+/+}$ to generate littermate PAK1$^{-/-}$;PAK2$^{fl/fl}$;MyoD$^{iCre/+}$ (referred to as 1/m2 dKO), PAK1$^{-/-}$;PAK2$^{fl/fl}$;MyoD$^{+/+}$ (referred to as PAK1 KO), PAK1$^{+/-}$;PAK2$^{fl/fl}$;MyoD$^{iCre/+}$ (referred to as PAK2 mKO), and PAK1$^{+/-}$;PAK2$^{fl/fl}$;MyoD$^{+/+}$ (referred to as controls) used for experiments. Female and male mice were used for measurement of insulin-stimulated glucose uptake in isolated muscle. The mice were 10-16 weeks of age at the time of tissue dissection and glucose uptake measurements. Number of mice in each group: Control, *n = 6/4* (female/male); PAK1 KO, *n = 5/4*, PAK2 mKO, *n = 6/4*, d1/2KO, *n = 6/3*. Another cohort of mice was used for whole-body metabolic measurements. The first measurement (insulin tolerance) was at 11-24 weeks of age and the last measurement was at 23-33 weeks of age (home cage calorimetry). Number of mice in each group: Control, *n = 9/11* (female/male); PAK1 KO, *n = 8/10*, PAK2 mKO, *n = 12/9*, d1/2KO, *n = 9/14*. For some of the metabolic measurements, only a subgroup of mice was used as indicated in the relevant figure legends. Mice received standard rodent chow diet and water ad libitum.

All animals were maintained on a 12:12-hour light-dark cycle and housed at 22°C (with allowed fluctuation of ±2°C) with nesting material. The mice were group-housed. All animal experiments complied with the European Convention for the protection of vertebrate animals used for experimental and other scientific purposes (No. 123, Strasbourg, France, 1985) and were approved by the Danish Animal Experimental Inspectorate.

Body composition. Body composition was analyzed using magnetic resonance imaging (EchoMRI-4in1TM, Echo Medical System LLC, Texas, USA). Chow-fed PAK1 KO and control littermates were assessed at 7-19 weeks of age. HFD-fed PAK1 KO and control littermates were assessed 18-19 weeks into the diet intervention (24-34 weeks of age). Chow-fed PAK1 KO, PAK2 mKO, 1/m2 dKO mice and control littermates were assessed at 16-29 weeks of age.

Glucose tolerance test (GTT). Prior to the test, chow- and HFD-fed PAK1 KO mice and control littermates fasted for 12 hours from 10 p.m, while chow-fed PAK1 KO, PAK2 mKO, 1/m2 dKO mice and control littermates fasted for 6 hours from 6 a.m. D-mono-glucose (2 g kg^{-1} body weight) was administered intraperitoneal (i.p) and blood was collected from the tail vein and blood glucose concentration determined at the indicated time points using a glucometer (Bayer Contour, Bayer, Switzerland). Incremental Area Under the Curve (AUC) from the basal blood glucose concentration was determined using the trapezoid rule. For measurement of plasma insulin, glucose was administered i.p. on a separate experimental day (1-2 weeks after the GTT) and blood was sampled at time points 0 and 20 minutes, centrifuged and plasma was quickly frozen in liquid nitrogen and stored at -20°C until processing. Plasma insulin was analyzed in duplicate (Mouse Ultrasensitive Insulin ELISA, #80-INSTRU-E10, ALPCO Diagnostics, USA). Homeostatic model assessment of insulin resistance (HOMA-IR) was calculated according to the formula: Fasting plasma insulin (mU L^{-1}) X Fasting blood glucose (mM)/22.5. Glucose tolerance was assessed in 8-20 weeks of age chow-fed PAK1 KO mice and in week 14 of the diet intervention of HFD-fed PAK1 KO mice (20-30 weeks of age). In chow-fed PAK1 KO, PAK2 mKO, 1/m2 dKO mice and control littermates, glucose tolerance was assessed at 13-26 weeks of age.

Insulin tolerance test (ITT). Prior to the test, chow-fed PAK1 KO, PAK2 mKO, 1/m2 dKO mice and control littermates fasted for 4 hours from 6 a.m. Insulin (0.5 U kg^{-1} body weight) was administered i.p. and blood was collected from the tail vein and blood glucose concentration

399 determined using a glucometer (Bayer Contour, Bayer, Switzerland) at time point 0, 15, 30, 60, 90
400 and 120 minutes. For two female control mice and four female PAK2 mKO mice, the ITT had to be
401 stopped before the 120'-time point due to hypoglycemia (blood glucose <1.2 mM). Thus, blood
402 glucose was not measured in these mice for the last couple of time points. Insulin tolerance was
403 assessed in 11-24 weeks of age chow-fed PAK1 KO, PAK2 mKO, 1/m2 dKO mice and control
404 littermates.

405 ***Home cage indirect calorimetry.*** One week prior to the calorimetric measurements, chow-fed
406 PAK1 KO, PAK2 mKO, 1/m2 dKO mice and control littermates were single-housed in specialized
407 cages for indirect gas calorimetry but uncoupled from the PhenoMaster indirect calorimetry system
408 (TSE PhenoMaster metabolic cage systems, TSE Systems, Germany). After a 2-day acclimation
409 period coupled to the PhenoMaster indirect calorimetry system, oxygen consumption, CO_2
410 production, habitual activity (beam breaks) and food intake were measured for 72 hours (TSE
411 LabMaster V5.5.3, TSE Systems, Germany). On day 2, mice fasted during the dark period followed
412 by refeeding on day 3. Respiratory exchange ratio (RER) was calculated as the ratio between CO_2
413 production and oxygen consumption. The mice were 23-33 weeks of age.

414 ***Incubation of isolated muscles.*** Soleus and EDL muscles were dissected from anaesthetized mice
415 (6 mg pentobarbital sodium 100 g^{-1} body weight i.p.) and suspended at resting tension (4-5 mN) in
416 incubations chambers (Multi Myograph System, Danish Myo Technology, Denmark) in Krebs-
417 Ringer-Henseleit buffer with 2 mM pyruvate and 8 mM mannitol at 30°C, as described previously
418 [49]. Additionally, the Krebs-Ringer-Henseleit buffer was supplemented with 0.1% BSA (v/v).
419 Isolated muscles from female C57BL/6J mice were pre-incubated with 40 µM IPA-3 (Sigma-
420 Aldrich) or as a control DMSO (0.25%) for 25 minutes followed by 30 minutes of insulin
421 stimulation (60 nM; Actrapid, Novo Nordisk, Denmark). Isolated muscles from chow-PAK1 KO
422 were pre-incubated for 30 minutes followed by 30 minutes of insulin stimulation (0.6 nm or 60

nM). Isolated muscles from chow-fed PAK1 KO, PAK2 mKO, 1/m2 dKO mice or control littermates were pre-incubated for 20 minutes followed by 20 minutes of insulin stimulation (60 nM). 2DG uptake was measured together with 1 mM 2DG during the last 10 min of the insulin stimulation period using 0.6 μCi mL^{-1} [^{3}H]-2DG and 0.180 μCi mL^{-1} [^{14}C]-mannitol radioactive tracers as described previously [49]. Tissue-specific [^{3}H]-2DG accumulation with [^{14}C]-mannitol as an extracellular marker was determined as previously described [50].

In vivo insulin-stimulated 2-Deoxyglucose uptake in PAK1 KO mice during a r.o. ITT. To determine 2DG uptake in skeletal muscle of PAK1 KO mice and littermate controls, [^{3}H]-2DG (Perkin Elmer) was administered retro-orbitally (r.o.) in a bolus of saline containing 66.7 μCi mL^{-1} [^{3}H]-2DG (~32.4 Ci/mmol) corresponding to ~10 μCi/mouse in chow-fed mice or ~15 μCi/mouse in HFD-fed mice (6 μL g^{-1} body weight) as described [17]. The [^{3}H]-2DG saline bolus was with or without insulin (Actrapid, Novo Nordisk, Denmark). Decreased insulin clearance has been observed by us [17] and others in obese rodent [51,52] and human [53] models. Therefore, to correct for changes in insulin clearance, 0.5 U kg^{-1} body weight of insulin was administered in chow-fed mice whereas only 60% of this dosage was administered to HFD-fed mice. Prior to stimulation, mice fasted for 4 hours from 07:00 and were anaesthetized (7.5/9 mg [Chow/HFD] pentobarbital sodium 100 g^{-1} body weight i.p.) 15 minutes before the r.o. injection. Blood samples were collected from the tail vein after the r.o. injection and analyzed for glucose concentration using a glucometer (Bayer Contour, Bayer, Switzerland) at the time points 0, 5 and 10 minutes. After 10 minutes, skeletal muscle (gastrocnemius, quadriceps, triceps brachii and soleus) were excised, rinsed in saline, and quickly frozen in liquid nitrogen and stored at -80°C until processing. Blood was collected by punctuation of the heart, centrifuged and plasma was quickly frozen in liquid nitrogen and stored at -80°C until processing. Plasma samples were analyzed for insulin concentration and specific [^{3}H]-2DG activity. Plasma insulin was analyzed in duplicate (Mouse Ultrasensitive Insulin

ELISA, #80-INSTRU-E10, ALPCO Diagnostics, USA). Tissue-specific 2DG-6-phosphate accumulation was measured as described [54,55]. To determine 2DG clearance from the plasma into the specific tissue, tissue-specific [^{3}H]-2DG-6-P was divided by AUC of the plasma-specific [^{3}H]-2DG activity at the time points 0 and 10 minutes. To estimate tissue-specific glucose uptake (glucose uptake index), clearance was multiplied by the average blood glucose levels for the time points 0, 5, and 10 minutes. Tissue-specific 2DG clearance and glucose uptake were related to analyzed muscle tissue weight and time.

Muscle analyses. Prior to homogenization, gastrocnemius, quadriceps, and triceps brachii muscles were pulverized in liquid nitrogen. All muscle were homogenized 2 x 30 sec at 30 Hz using a Tissuelyser II (Qiagen, USA) in ice-cold homogenization buffer (10% (v/v) Glycerol, 1% (v/v) NP-40, 20 mM Na-pyrophosphate, 150 mM NaCl, 50 mM HEPES (pH 7.5), 20 mM β-glycerophosphate, 10 mM NaF, 2mM PMSF, 1 mM EDTA (pH 8.0), 1 mM EGTA (pH 8.0), 2 mM Na3VO4, 10 µg mL^{-1} Leupeptin, 10 µg mL^{-1} Aprotinin, 3 mM Benzamidine). After rotation end-over-end for 30 min at 4°C, lysate supernatants were collected by centrifugation (10,854-15,630 x g) for 15-20 min at 4°C.

Immunoblotting. Lysate protein concentration was determined using the bicinchoninic acid (BCA) method using BSA standards and BCA assay reagents (Pierce). Immunoblotting samples were prepared in 6x sample buffer (340 mM Tris (pH 6.8), 225 mM DTT, 11% (w/v) SDS, 20% (v/v) Glycerol, 0.05% (w/v) Bromphenol blue). Protein phosphorylation (p) and total protein expression were determined by standard immunoblotting technique loading equal amounts of protein. The polyvinylidene difluoride membrane (Immobilon Transfer Membrane; Millipore) was blocked in Tris-Buffered Saline with added Tween20 (TBST) and 2% (w/v) skim milk or 5% (w/v) BSA protein for 15 minutes at room temperature, followed by incubation overnight at 4°C with a primary antibody (Table 1). Next, the membrane was incubated with horseradish peroxidase-conjugated

secondary antibody (Jackson Immuno Research) for 1 hour at room temperature. Bands were visualized using Bio-Rad ChemiDocTM MP Imaging System and enhanced chemiluminescence (ECL+; Amersham Biosciences). Densitometric analysis was performed using Image LabTM Software, version 4.0 (Bio-Rad, USA). Coomassie brilliant blue staining was used as a loading control [56].

Statistical analyses. Data are presented as mean ± S.E.M. or when applicable mean ± S.E.M. with individual data points shown. Statistical tests varied according to the dataset being analyzed and the specific tests used are indicated in the figure legends. If the null hypothesis was rejected, Tukey's post hoc test was used to evaluate significant main effects of genotype and significant interactions in ANOVAs. $P < 0.05$ was considered statistically significant. $P<0.1$ was considered a tendency. Except for mixed-effects model analyses performed in GraphPad Prism, version 8.2.1. (GraphPad Software, La Jolla, CA, USA), all statistical analyses were performed using Sigma Plot, version 13 (Systat Software Inc., Chicago, IL, USA). Due to missing values ascribed to hypoglycemia, differences between genotypes and the effect of insulin administration were assessed with a mixed-effects model analysis in Fig. 5F and S5F.

Disclosure summary

No potential conflicts of interest relevant to this article were reported.

Acknowledgements

We thank our colleagues, especially Jørgen Wojtaszewski and Bente Kiens, at the Section of Molecular Physiology, Department of Nutrition, Exercise, and Sports (NEXS), Faculty of Science,

University of Copenhagen, for fruitful discussions on this topic. We acknowledge the skilled technical assistance of Betina Bolmgren, Irene B. Nielsen, and Mona Ali (Section of Molecular Physiology, NEXS, Faculty of Science, University of Copenhagen, Denmark). The PAK1 KO founder mice were a kind gift from Debbie Thurmond (Department of Molecular & Cellular Endocrinology, Diabetes and Metabolism Research Institute, City of Hope/BRICA, USA).

Author contributions

LLVM, EAR, and LS conceptualized and designed the study. LLVM and LS conducted the experiments and analyzed the data, with experimental contribution and/or interpretation of data from MJ, RK, GAJ, ABM, JRK, A-ML, NRA, PS, TEJ, RSK. LLVM, EAR, and LS drafted the manuscript. All authors contributed to the final version of the manuscript. All authors are guarantor of this work and take responsibility for the integrity of the data and the accuracy of the data analysis.

Grants

This study was supported by a PhD fellowship from The Lundbeck Foundation (grant 2015-3388 to LLVM); PhD scholarships from The Danish Diabetes Academy, funded by The Novo Nordisk Foundation (ABM and JRK); Postdoctoral research grant from the Danish Diabetes Academy, funded by the Novo Nordisk Foundation (grant NNF17SA0031406 to A-ML); National Institute of Arthritis and Musculoskeletal and Skin Diseases (grant AR046207 and AR070231 to RSK); The Danish Council for Independent Research, Medical Sciences (grant DFF-4004-00233 to LS, grant 6108-00203 to EAR); The Novo Nordisk Foundation (grant 10429 to EAR, grant 15182 to TEJ, grant NNF16OC0023418 and NNF18OC0032082 to LS).

516

517

518 **References**

519 1. DeFronzo RA, Gunnarsson R, Björkman O, Olsson M, Wahren J. Effects of insulin on peripheral and
520 splanchnic glucose metabolism in noninsulin-dependent (type II) diabetes mellitus. J Clin Invest.
521 1985;76: 149–155. doi:10.1172/JCI111938

522 2. Baron AD, Brechtel G, Wallace P, Edelman S V. Rates and tissue sites of non-insulin- and insulin-
523 mediated glucose uptake in humans. Am J Physiol Metab. 1988;255: E769–E774.
524 doi:10.1152/ajpendo.1988.255.6.E769

525 3. Samuel VT, Petersen KF, Shulman GI. Lipid-induced insulin resistance: unravelling the mechanism.
526 Lancet. 2010;375: 2267–2277. doi:10.1016/S0140-6736(10)60408-4

527 4. Lauritzen HPMM. Insulin- and Contraction-Induced Glucose Transporter 4 Traffic in Muscle. Exerc
528 Sport Sci Rev. 2013;41: 77–86. doi:10.1097/JES.0b013e318275574c

529 5. Tsakiridis T, Taha C, Grinsteinl S, Klip A. Insulin activates a p21-activated kinase in muscle cells via
530 phosphatidylinositol 3-kinase. J Biol Chem. 1996;271: 19664–19667. doi:10.1074/jbc.271.33.19664

531 6. Tunduguru R, Chiu TT, Ramalingam L, Elmendorf JS, Klip A, Thurmond DC. Signaling of the p21-
532 activated kinase (PAK1) coordinates insulin-stimulated actin remodeling and glucose uptake in
533 skeletal muscle cells. Biochem Pharmacol. 2014;92: 380–388. doi:10.1016/j.bcp.2014.08.033

534 7. Wang Z, Oh E, Clapp DW, Chernoff J, Thurmond DC. Inhibition or ablation of p21-activated kinase
535 (PAK1) disrupts glucose homeostatic mechanisms in vivo. J Biol Chem. 2011;286: 41359–41367.
536 doi:10.1074/jbc.M111.291500

537 8. Joseph GA, Lu M, Radu M, Lee JK, Burden SJ, Chernoff J, et al. Group I Paks Promote Skeletal
538 Myoblast Differentiation In Vivo and In Vitro. Mol Cell Biol. 2017;37: e00222-16.
539 doi:10.1128/MCB.00222-16

540 9. Chiang YA, Jin T. p21-Activated protein kinases and their emerging roles in glucose homeostasis.
541 Am J Physiol Metab. 2014;306: E707–E722. doi:10.1152/ajpendo.00506.2013

542 10. Manser E, Leung T, Salihuddin H, Zhao Z, Lim L. A brain serine/threonine protein kinase activated
543 by Cdc42 and Rac1. Nature. 1994;367: 40–46. doi:10.1038/367040a0

544 11. Arvidson AR. A tale of two parks. Landsc Archit. 2008;98: 108–117. doi:10.1042/bc20070109

545 12. Khayat ZA, Tong P, Yaworsky K, Bloch RJ, Klip A. Insulin-induced actin filament remodeling
546 colocalizes actin with phosphatidylinositol 3-kinase and GLUT4 in L6 myotubes. J Cell Sci.
547 2000;113 Pt 2: 279–90. Available: http://www.ncbi.nlm.nih.gov/pubmed/10633079

548 13. JeBailey L, Wanono O, Niu W, Roessler J, Rudich A, Klip A. Ceramide- and oxidant-induced insulin
549 resistance involve loss of insulin-dependent Rac-activation and actin remodeling in muscle cells.
550 Diabetes. 2007;56: 394–403. doi:10.2337/db06-0823

551 14. Ueda S, Kitazawa S, Ishida K, Nishikawa Y, Matsui M, Matsumoto H, et al. Crucial role of the small
552 GTPase Rac1 in insulin-stimulated translocation of glucose transporter 4 to the mouse skeletal muscle
553 sarcolemma. FASEB J. 2010;24: 2254–2261. doi:10.1096/fj.09-137380

554 15. Sylow L, Jensen TE, Kleinert M, Hojlund K, Kiens B, Wojtaszewski J, et al. Rac1 Signaling Is
555 Required for Insulin-Stimulated Glucose Uptake and Is Dysregulated in Insulin-Resistant Murine and
556 Human Skeletal Muscle. Diabetes. 2013;62: 1865–1875. doi:10.2337/db12-1148

16. Sylow L, Kleinert M, Pehmøller C, Prats C, Chiu TT, Klip A, et al. Akt and Rac1 signaling are jointly required for insulin-stimulated glucose uptake in skeletal muscle and downregulated in insulin resistance. Cell Signal. 2014;26: 323–331. doi:10.1016/j.cellsig.2013.11.007

17. Raun SH, Ali M, Kjøbsted R, Møller LL V, Federspiel MA, Richter EA, et al. Rac1 muscle knockout exacerbates the detrimental effect of high-fat diet on insulin-stimulated muscle glucose uptake independently of Akt. J Physiol. 2018;596: 2283–2299. doi:10.1113/JP275602

18. Sano H, Kane S, Sano E, Mîinea CP, Asara JM, Lane WS, et al. Insulin-stimulated Phosphorylation of a Rab GTPase-activating Protein Regulates GLUT4 Translocation. J Biol Chem. 2003;278: 14599–14602. doi:10.1074/jbc.C300063200

19. Thong FSL, Dugani CB, Klip A. Turning signals on and off: GLUT4 traffic in the insulin-signaling highway. Physiology. American Physiological Society; 2005. pp. 271–284. doi:10.1152/physiol.00017.2005

20. Kramer HF, Witczak CA, Taylor EB, Fujii N, Hirshman MF, Goodyear LJ. AS160 Regulates Insulin- and Contraction-stimulated Glucose Uptake in Mouse Skeletal Muscle. J Biol Chem. 2006;281: 31478–31485. doi:10.1074/jbc.M605461200

21. Benner GE, Dennis PB, Masaracchia RA. Activation of an S6/H4 Kinase (PAK 65) from Human Placenta by Intramolecular and Intermolecular Autophosphorylation. J Biol Chem. 1995;270: 21121–21128. doi:10.1074/jbc.270.36.21121

22. Gatti A, Huang Z, Tuazon PT, Traugh JA. Multisite autophosphorylation of p21-activated protein kinase gamma-PAK as a function of activation. J Biol Chem. 1999;274: 8022–8. doi:10.1074/jbc.274.12.8022

23. Stierwalt HD, Ehrlicher SE, Bergman BC, Robinson MM, Newsom SA. Insulin-stimulated Rac1-GTP binding is not impaired by palmitate treatment in L6 myotubes. Physiol Rep. 2018;6: e13956. doi:10.14814/phy2.13956

24. Chiang YA, Shao W, Xu XX, Chernoff J, Jin T. P21-activated protein kinase 1 (Pak1) mediates the cross talk between insulin and β-catenin on proglucagon gene expression and its ablation affects glucose homeostasis in male C57BL/6 mice. Endocrinology. 2013;154: 77–88. doi:10.1210/en.2012-1781

25. Chiu TT, Patel N, Shaw AE, Bamburg JR, Klip A. Arp2/3- and Cofilin-coordinated Actin Dynamics Is Required for Insulin-mediated GLUT4 Translocation to the Surface of Muscle Cells. Blanchoin L, editor. Mol Biol Cell. 2010;21: 3529–3539. doi:10.1091/mbc.e10-04-0316

26. Tunduguru R, Zhang J, Aslamy A, Salunkhe VA, Brozinick JT, Elmendorf JS, et al. The actin-related p41ARC subunit contributes to p21-activated kinase-1 (PAK1)-mediated glucose uptake into skeletal muscle cells. J Biol Chem. 2017;292: 19034–19043. doi:10.1074/jbc.M117.801340

27. Wasserman DH, Kang L, Ayala JE, Fueger PT, Lee-Young RS. The physiological regulation of glucose flux into muscle in vivo. J Exp Biol. 2011;214: 254–262. doi:10.1242/jeb.048041

28. Hansen PA, Gulve EA, Marshall BA, Gao J, Pessin JE, Holloszy JO, et al. Skeletal muscle glucose transport and metabolism are enhanced in transgenic mice overexpressing the Glut4 glucose transporter. J Biol Chem. 1995;270: 1679–84. doi:10.1074/jbc.270.5.1679

29. Hansen PA, Marshall BA, Chen M, Holloszy JO, Mueckler M. Transgenic Overexpression of Hexokinase II in Skeletal Muscle Does Not Increase Glucose Disposal in Wild-type or Glut1-overexpressing Mice. J Biol Chem. 2000;275: 22381–22386. doi:10.1074/jbc.M001946200

30. Zisman A, Peroni OD, Abel ED, Michael MD, Mauvais-Jarvis F, Lowell BB, et al. Targeted disruption of the glucose transporter 4 selectively in muscle causes insulin resistance and glucose intolerance. Nat Med. 2000;6: 924–928. doi:10.1038/78693

31. Deacon SW, Beeser A, Fukui JA, Rennefahrt UEE, Myers C, Chernoff J, et al. An Isoform-Selective, Small-Molecule Inhibitor Targets the Autoregulatory Mechanism of p21-Activated Kinase. Chem Biol. 2008;15: 322–331. doi:10.1016/j.chembiol.2008.03.005

32. Davies SP, Reddy H, Caivano M, Cohen P. Specificity and mechanism of action of some commonly used protein kinase inhibitors. Biochem J. 2000;351: 95–105. doi:10.1517/13543776.11.3.405

33. Ahn M, Yoder SM, Wang Z, Oh E, Ramalingam L, Tunduguru R, et al. The p21-activated kinase (PAK1) is involved in diet-induced beta cell mass expansion and survival in mice and human islets. Diabetologia. 2016;59: 2145–2155. doi:10.1007/s00125-016-4042-0

34. Joseph GA, Hung M, Goel AJ, Hong M, Rieder M-K, Beckmann ND, et al. Late-onset megaconial myopathy in mice lacking group I Paks. Skelet Muscle. 2019;9: 5. doi:10.1186/s13395-019-0191-4

35. Lansey MN, Walker NN, Hargett SR, Stevens JR, Keller SR. Deletion of Rab GAP AS160 modifies glucose uptake and GLUT4 translocation in primary skeletal muscles and adipocytes and impairs glucose homeostasis. Am J Physiol Metab. 2012;303: E1273–E1286. doi:10.1152/ajpendo.00316.2012

36. Wang HY, Ducommun S, Quan C, Xie B, Li M, Wasserman DH, et al. AS160 deficiency causes whole-body insulin resistance via composite effects in multiple tissues. Biochem J. 2013;449: 479–489. doi:10.1042/BJ20120702

37. Somwar R, Niu W, Kim DY, Sweeney G, Randhawa VK, Huang C, et al. Differential Effects of Phosphatidylinositol 3-Kinase Inhibition on Intracellular Signals Regulating GLUT4 Translocation and Glucose Transport. J Biol Chem. 2001;276: 46079–46087. doi:10.1074/jbc.M109093200

38. Somwar R, Kim DY, Sweeney G, Huang C, Niu W, Lador C, et al. GLUT4 translocation precedes the stimulation of glucose uptake by insulin in muscle cells: potential activation of GLUT4 via p38 mitogen-activated protein kinase. Biochem J. 2001;359: 639–49. doi:10.1042/0264-6021:3590639

39. Funaki M, Randhawa P, Janmey PA. Separation of Insulin Signaling into Distinct GLUT4 Translocation and Activation Steps. Mol Cell Biol. 2004;24: 7567–7577. doi:10.1128/mcb.24.17.7567-7577.2004

40. Lund S, Holman GD, Zierath JR, Rincon J, Nolte LA, Clark AE, et al. Effect of Insulin on GLUT4 CeU Surface Content and Turnover Rate in Human Skeletal Muscle as Measured by the Exofacial Bis-Mannose Photolabeling Technique. 1965.

41. Nozaki S, Ueda S, Takenaka N, Kataoka T, Satoh T. Role of RalA downstream of Rac1 in insulin-dependent glucose uptake in muscle cells. Cell Signal. 2012;24: 2111–2117. doi:10.1016/j.cellsig.2012.07.013

42. Takenaka N, Sumi Y, Matsuda K, Fujita J, Hosooka T, Noguchi T, et al. Role for RalA downstream of Rac1 in skeletal muscle insulin signalling. Biochem J. 2015;469: 445–54. doi:10.1042/BJ20150218

43. Bedard K, Krause K-H. The NOX Family of ROS-Generating NADPH Oxidases: Physiology and Pathophysiology. Physiol Rev. 2007;87: 245–313. doi:10.1152/physrev.00044.2005

44. Abo A, Pick E, Hall A, Totty N, Teahan CG, Segal AW. Activation of the NADPH oxidase involves the small GTP-binding protein p21rac1. Nature. 1991;353: 668–670. doi:10.1038/353668a0

45. Contreras-Ferrat A, Llanos P, Vásquez C, Espinosa A, Osorio-Fuentealba C, Arias-Calderon M, et al. Insulin elicits a ROS-activated and an IP3-dependent Ca2+ release, which both impinge on GLUT4 translocation. J Cell Sci. 2014;127: 1911–1923. doi:10.1242/jcs.138982

46. Henríquez-Olguin C, Knudsen JR, Raun SH, Li Z, Dalbram E, Treebak JT, et al. Cytosolic ROS production by NADPH oxidase 2 regulates muscle glucose uptake during exercise. Nat Commun. 2019;10: 4623. doi:10.1038/s41467-019-12523-9

47. Sylow L, Jensen TE, Kleinert M, Mouatt JR, Maarbjerg SJ, Jeppesen J, et al. Rac1 Is a Novel Regulator of Contraction-Stimulated Glucose Uptake in Skeletal Muscle. Diabetes. 2013;62: 1139–1151. doi:10.2337/db12-0491

48. Allen JD, Jaffer ZM, Park SJ, Burgin S, Hofmann C, Sells MA, et al. P21-activated kinase regulates mast cell degranulation via effects on calcium mobilization and cytoskeletal dynamics. Blood. 2009;113: 2695–2705. doi:10.1182/blood-2008-06-160861

49. Viollet B, Andreelli F, Jørgensen SB, Perrin C, Geloen A, Flamez D, et al. The AMP-activated protein kinase α2 catalytic subunit controls whole-body insulin sensitivity. J Clin Invest. 2003;111: 91–98. doi:10.1172/JCI16567

50. Kjøbsted R, Treebak JT, Fentz J, Lantier L, Viollet B, Birk JB, et al. Prior AICAR stimulation increases insulin sensitivity in mouse skeletal muscle in an AMPK-dependent manner. Diabetes. 2015;64: 2042–2055. doi:10.2337/db14-1402

51. Strömblad G, Björntorp P. Reduced hepatic insulin clearance in rats with dietary-induced obesity. Metabolism. 1986;35: 323–327. doi:10.1016/0026-0495(86)90148-4

52. Brandimarti P, Costa-Júnior JM, Ferreira SM, Protzek AO, Santos GJ, Carneiro EM, et al. Cafeteria diet inhibits insulin clearance by reduced insulindegrading enzyme expression and mRNA splicing. J Endocrinol. 2013;219: 173–182. doi:10.1530/JOE-13-0177

53. Jung S-H, Jung C-H, Reaven GM, Kim SH. Adapting to insulin resistance in obesity: role of insulin secretion and clearance. Diabetologia. 2018;61: 681–687. doi:10.1007/s00125-017-4511-0

54. Ferre P, Leturque A, Burnol A-F, Penicaud L, Girard J. A method to quantify glucose utilization in vivo in skeletal muscle and white adipose tissue of the anaesthetized rat. Biochem J. 1985;228: 103–110.

55. Fueger PT, Bracy DP, Malabanan CM, Pencek RR, Wasserman DH. Distributed control of glucose uptake by working muscles of conscious mice: roles of transport and phosphorylation. Am J Physiol Metab. 2004;286: E77–E84. doi:10.1152/ajpendo.00309.2003

56. Welinder C, Ekblad L. Coomassie Staining as Loading Control in Western Blot Analysis. J Proteome Res. 2011;10: 1416–1419. doi:10.1021/pr1011476

Figure Legends

Figure 1: Insulin-stimulated glucose uptake is reduced in IPA-3-treated mouse soleus muscle. **(A-B)** Insulin-stimulated (60 nM) 2-Deoxyglucose (2DG) uptake in isolated soleus (A) and extensor digitorum longus (EDL, B) muscle ± 40 µM IPA-3 or as a control DMSO (0.25%). Isolated muscles were pre-incubated for 25 minutes followed by 30 minutes of insulin stimulation with 2DG uptake analyzed for the final 10 minutes of stimulation. **(C-H)** Quantification of phosphorylated (p)PAK1 T423, pAkt T308, and pAkt S473 in insulin-stimulated soleus (C, E, and G) and EDL (D, F, and H) muscle ± 40 µM IPA-3 or as a control DMSO (0.25%). Some of the data points were excluded due to the quality of the immunoblot, and the number of determinations was *n = 8/7* for pAkt S473 and T308 in soleus muscle. **(I-J)** Representative blots showing pPAK1 T423, pAkt T308, and pAkt S473 in soleus (I) and EDL (J) muscle. Statistics were evaluated with a two-way repeated measures (RM) ANOVA. Main effects are indicated in the panels. Interactions in two-way RM ANOVA were evaluated by Tukey's post hoc test: Insulin stimulation vs. basal **/*** ($p<0.01/0.001$); IPA-3 vs. DMSO (#)/#/##/### ($p<0.1/0.05/0.01/0.001$). Unless otherwise stated previously in the figure legend, the number of determinations in each group: Soleus, *n = 9/8* (DMSO/IPA-3); EDL, *n = 9/8*. Data are presented as mean ± S.E.M. with individual data points shown. Paired data points are connected with a straight line. A.U., arbitrary units.

Figure 2: PAK1 knockout does not affect whole-body glucose homeostasis or insulin-stimulated glucose uptake in isolated skeletal muscle. (A) Representative blots showing PAK1 protein expression in gastrocnemius, quadriceps, and triceps brachii muscle from PAK1 knockout (KO) mice or control littermates. **(B)** Body composition (FM: Fat mass; LBM: Lean body mass; BW: Body weight) in gram in chow-fed PAK1 KO mice (*n = 12*) or control littermates (*n = 13*). The mice were 7-19 weeks of age. Statistics were evaluated with a Student's t-test. **(C)** Energy intake in chow-fed PAK1 KO mice (*n = 8*) or control littermates (*n = 8*). Energy intake was

monitored in a separate cohort of mice. Statistics were evaluated with a Student's t-test. **(D)** Blood glucose levels during a glucose tolerance test (GTT) in chow-fed PAK1 KO mice (*n = 9*) or control littermates (*n = 10*). The mice were 8-20 weeks of age. Statistics were evaluated with a two-way repeated measures (RM) ANOVA. **(E)** Incremental Area Under the Curve (AUC) for blood glucose levels during the GTT in panel D. Statistics were evaluated with a Student's t-test. **(F)** Plasma insulin values during a GTT in chow-fed PAK1 KO mice (*n = 10*) or control littermates (*n = 13*). The mice were 9-21 weeks of age. Statistics were evaluated with a two-way RM measures ANOVA. **(G)** Homeostatic Model Assessment of Insulin Resistance (HOMA-IR) in chow-fed PAK1 KO mice (*n=10*) or control littermates (*n=13*). Statistics were evaluated with a Student's t-test. **(H-I)** Submaximal (0.6 nM) and maximal (60 nM) insulin-stimulated 2-Deoxyglucose (2DG) uptake in isolated soleus (H) and extensor digitorum longus (EDL; I) muscle from PAK1 KO mice or littermate controls. Isolated muscles were pre-incubated for 30 minutes followed by 30 minutes of insulin stimulation with 2DG uptake analyzed for the final 10 minutes of stimulation. The mice were 12-24 weeks of age. The number of determinations in each group: Soleus-Control, *n = 6/7* (Submax/max); Soleus-PAK1 KO, *n = 7/7*; EDL-Control, *n = 6/6*; EDL-PAK1 KO, *n = 7/7*. Statistics were evaluated with two two-way RM measures ANOVA. Main effects are indicated in the panels. Data are presented as mean ± S.E.M. or when applicable mean ± S.E.M. with individual data points shown. Paired data points are connected with a straight line.

Figure 3: PAK1 is dispensable for *in vivo* insulin-stimulated glucose uptake in mouse skeletal muscle. (A-B) Blood glucose levels during a retro-orbital insulin tolerance test (r.o. ITT) in chow- (A) and HFD-fed (B) PAK1 knockout (KO) mice or control littermates. Chow-fed mice were investigated at 10-24 weeks of age. Mice fed a 60E% high-fat diet (HFD) for 21 weeks were investigated at 27-37 weeks of age. The number of mice in each group: Chow, *n = 12/6* (Control/PAK1 KO); HFD, *n = 10/11*. Statistics were evaluated with a two-way repeated measures

ANOVA. **(C-D)** Insulin-stimulated (Chow: 0.5 U kg^{-1} body weight; HFD: 60% of insulin administered to chow-fed mice) glucose uptake index in gastrocnemius (Gast), quadriceps (Quad), triceps brachii (Triceps) and soleus muscle from chow- (C) and HFD-fed (D) PAK1 KO mice or control littermates. The number of mice in each group: Chow-Saline, *n = 12/4* (Control/PAK1 KO); Chow-Insulin, *n = 12/6*; HFD-Saline, *n = 6/6*; HFD-Insulin, *n = 10/11*. Statistics were evaluated with a two-way ANOVA for each of the muscles. Main effects are indicated in the panels. Data are presented as mean ± S.E.M. or when applicable mean ± S.E.M. with individual data points shown.

Figure 4: Whole-body energy utilization is unaffected by whole-body genetic ablation of PAK1 and muscle-specific genetic ablation of PAK2. (A) Representative blots showing PAK1and PAK2 protein expression in soleus and extensor digitorum longus (EDL) muscle from chow-fed whole-body PAK1 knockout (KO), muscle-specific PAK2 (m)KO, PAK1/2 double KO (d1/2KO) mice or control littermates. **(B)** Body weight of chow-fed PAK1 KO (*n = 18*), PAK2 mKO (*n = 21*), 1/m2 dKO mice (*n = 23*) or control littermates (*n = 20*). The mice were 16-29 weeks of age. Statistics were evaluated with a two-way ANOVA to test the factors 'PAK1' (PAK1+/- vs. PAK-/-) and 'PAK2' ($PAK2^{fl/fl}$;$MyoD^{+/+}$ vs. $PAK2^{fl/fl}$;$MyoD^{iCre/+}$) thereby assessing the relative contribution of PAK1 and PAK2, respectively. Differences between genotypes were evaluated with one-way ANOVA. **(C)** Body composition (FM: Fat mass; LBM: Lean body mass) in gram in chow-fed PAK1 KO (*n = 18*), PAK2 mKO (*n = 21*), 1/m2 dKO mice (*n = 23*) or control littermates (*n = 20*). Statistics were evaluated with a two-way ANOVA to test the factors 'PAK1' (PAK1+/- vs. PAK-/-) and 'PAK2' ($PAK2^{fl/fl}$;$MyoD^{+/+}$ vs. $PAK2^{fl/fl}$;$MyoD^{iCre/+}$) thereby assessing the relative contribution of PAK1 and PAK2, respectively. Differences between genotypes were evaluated with a one-way ANOVA. **(D-G)** Oxygen uptake (VO_2; D), respiratory exchange ratio (RER; E), activity (beam breaks; F), and energy intake (G), in chow-fed PAK1 KO (*n = 11*), PAK2 mKO (*n = 11*), 1/m2 dKO mice (*n = 13*) or control littermates (*n = 8;* for energy intake, *n = 7*)

during the light and dark period recorded over a period of 72 hours. On day 2, the mice were fasted during the dark period and then refed on day 3. The mice were 23-33 weeks of age. Statistics were evaluated with two two-way ANOVAs to test the factors 'PAK1' (PAK1+/- vs. PAK-/-) and 'PAK2' ($PAK2^{fl/fl}$;$MyoD^{+/+}$ vs. $PAK2^{fl/fl}$;$MyoD^{iCre/+}$) in the light and dark period of day 1, respectively. Statistics for day 2 and 3 were evaluated similarly thereby assessing the relative contribution of PAK1 and PAK2. Differences between genotypes and the effect of the light and dark period were assessed with three two-way repeated measures (RM) ANOVA to test the factors 'Genotype' (Control vs. PAK1 KO vs. PAK2 mKO vs. 1/m2 dKO) and 'Period' (Light vs. Dark) at day 1, 2 and 3, respectively. Main effects are indicated in the panels. Significant one-way ANOVA and interactions in two-way (RM when applicable) ANOVA were evaluated by Tukey's post hoc test: Light vs. dark period */**/*** ($p<0.05/0.01/0.001$); Control vs. 1/m2 dKO †/††† ($p<0.05/0.001$); PAK1 KO vs. 1/m2 dKO ‡/‡‡/‡‡‡ ($p<0.05/0.01/0.001$); PAK2 mKO vs. 1/m2 dKO ($)/$/$$ ($p<0.1/0.05/0.01$). Data are presented as mean ± S.E.M. or when applicable mean ± S.E.M. with individual data points shown.

Figure 5: Mice lacking PAK2 in skeletal muscle are slightly glucose intolerant. (A) Blood glucose concentration in the fed state (8 a.m.) in chow-fed whole-body PAK1 knockout (KO) (*n = 18*), muscle-specific PAK2 (m)KO (*n = 21*), PAK1/2 double KO (d1/2KO) mice (*n = 23*) or control littermates (*n = 20*). The mice were 17-30 weeks of age. Statistics were evaluated with a two-way ANOVA to test the factors 'PAK1' (PAK1+/- vs. PAK-/-) and 'PAK2' ($PAK2^{fl/fl}$;$MyoD^{+/+}$ vs. $PAK2^{fl/fl}$;$MyoD^{iCre/+}$) thereby assessing the relative contribution of PAK1 and PAK2, respectively. Differences between genotypes were evaluated with a one-way ANOVA. **(B)** Blood glucose levels during a glucose tolerance test (GTT) in chow-fed PAK1 KO (*n = 18*), PAK2 mKO (*n = 19*), 1/m2 dKO mice (*n = 21*) or control littermates (*n = 19*). The mice were 13-26 weeks of age. Statistics were evaluated with six two-way ANOVAs to test the factors 'PAK1' (PAK1+/- vs. PAK-/-) and

'PAK2' ($PAK2^{fl/fl}$;$MyoD^{+/+}$ vs. $PAK2^{fl/fl}$;$MyoD^{iCre/+}$) at time point 0, 15, 30, 60, 90 and 120, respectively, thereby assessing the relative contribution of PAK1 and PAK2. Differences between genotypes and the effect of glucose administration were assessed with a two-way repeated measures (RM) ANOVA to test the factors 'Genotype' (Control vs. PAK1 KO vs. PAK2 mKO vs. 1/m2 dKO) and 'Time' (0 vs. 15 vs. 30 vs. 60 vs. 90 vs. 120). **(C)** Incremental Area Under the Curve (AUC) for blood glucose levels during the GTT in panel B. Statistics were evaluated with a two-way ANOVA to test the factors 'PAK1' (PAK1+/- vs. PAK-/-) and 'PAK2' ($PAK2^{fl/fl}$;$MyoD^{+/+}$ vs. $PAK2^{fl/fl}$;$MyoD^{iCre/+}$) thereby assessing the relative contribution of PAK1 and PAK2, respectively. Differences between genotypes were evaluated with one-way ANOVA. **(D)** Plasma insulin values during a GTT in chow-fed PAK1 KO (*n = 17*), PAK2 mKO (*n = 19*), 1/m2 dKO mice (*n = 22*) or control littermates (*n = 19*). The mice were 15-28 weeks of age. Statistics were evaluated with two two-way ANOVAs to test the factors 'PAK1' (PAK1+/- vs. PAK-/-) and 'PAK2' ($PAK2^{fl/fl}$;$MyoD^{+/+}$ vs. $PAK2^{fl/fl}$;$MyoD^{iCre/+}$) at time point 0 and 20, respectively, thereby assessing the relative contribution of PAK1 and PAK2. Differences between genotypes and the effect of glucose administration were assessed with a two-way RM ANOVA to test the factors 'Genotype' (Control vs. PAK1 KO vs. PAK2 mKO vs. 1/m2 dKO) and 'Time' (0 vs. 20). **(E)** Homeostatic Model Assessment of Insulin Resistance (HOMA-IR) in chow-fed PAK1 KO (*n = 18*), PAK2 mKO (*n = 19*), 1/m2 dKO mice (*n = 22*) or control littermates (*n = 20*). Statistics were evaluated with a two-way ANOVA to test the factors 'PAK1' (PAK1+/- vs. PAK-/-) and 'PAK2' ($PAK2^{fl/fl}$;$MyoD^{+/+}$ vs. $PAK2^{fl/fl}$;$MyoD^{iCre/+}$) thereby assessing the relative contribution of PAK1 and PAK2, respectively. Differences between genotypes were evaluated with a one-way ANOVA. **(F)** Blood glucose levels related to the basal concentration during an insulin tolerance test (ITT) in chow-fed PAK1 KO (*n = 15*), PAK2 mKO (*n = 18*), 1/m2 dKO mice (*n = 21*) or control littermates (*n = 19*). The mice were 11-24 weeks of age. For two female control mice and four female PAK2 mKO mice,

the ITT had to be stopped before the 120'-time point due to hypoglycemia (blood glucose <1.2 mM), and thus blood glucose was not determined for these mice for the last couple of time points. Statistics were evaluated with five two-way ANOVAs to test the factors 'PAK1' (PAK1+/- vs. PAK-/-) and 'PAK2' ($PAK2^{fl/fl}$;$MyoD^{+/+}$ vs. $PAK2^{fl/fl}$;$MyoD^{iCre/+}$) at time point 15, 30, 60, 90 and 120, respectively, thereby assessing the relative contribution of PAK1 and PAK2. Differences between genotypes and the effect of insulin administration were assessed with a mixed-effects model analysis to test the factors 'Genotype' (Control vs. PAK1 KO vs. PAK2 mKO vs. 1/m2 dKO) and 'Time' (0 vs. 15 vs. 30 vs. 60 vs. 90 vs. 120). Main effects are indicated in the panels. Significant one-way ANOVA and interactions in two-way (RM when applicable) ANOVA were evaluated by Tukey's post hoc test: Effect of glucose/insulin administration vs. time point 0' */*** ($p<0.05/0.001$). Data are presented as mean ± S.E.M. or when applicable mean ± S.E.M. with individual data points shown. Paired data points are connected with a straight line.

Figure 6: Muscle-specific PAK2 knockout, but not knockout of PAK1, partly reduces glucose uptake in EDL muscle. (A-B) Insulin-stimulated (60 nM) 2-Deoxyglucose (2DG) uptake in isolated soleus (A) and extensor digitorum longus (EDL; B) muscle from whole-body PAK1 knockout (KO), muscle-specific PAK2 (m)KO, PAK1/2 double KO (d1/2KO) mice or control littermates. Isolated muscles were pre-incubated for 20 minutes followed by 20 minutes of insulin stimulation with 2DG uptake analyzed for the final 10 minutes of stimulation. The mice were 10-16 weeks of age. Statistics were evaluated with two two-way ANOVAs to test the factors 'PAK1' (PAK1+/- vs. PAK-/-) and 'PAK2' ($PAK2^{fl/fl}$;$MyoD^{+/+}$ vs. $PAK2^{fl/fl}$;$MyoD^{iCre/+}$) in basal and insulin-stimulated samples, respectively, thereby assessing the relative contribution of PAK1 and PAK2. Differences between genotypes and the effect of insulin stimulation were assessed with a two-way repeated measures (RM) ANOVA to test the factors 'Genotype' (Control vs. PAK1 KO vs. PAK2 mKO vs. 1/m2 dKO) and 'Stimuli' (Basal vs. Insulin). **(C-D)** Δ2DG uptake in soleus (C)

and EDL (D) muscle from panel C-D. Statistics were evaluated with a two-way ANOVA to test the factors 'PAK1' (PAK1+/- vs. PAK-/-) and 'PAK2' ($PAK2^{fl/fl}$;$MyoD^{+/+}$ vs. $PAK2^{fl/fl}$;$MyoD^{iCre/+}$) to assess of the relative contribution of PAK1 and PAK2, respectively. Differences between genotypes were evaluated with a one-way ANOVA. The number of determinations in each group: Control, *n = 9/10* (soleus/EDL); PAK1 KO, *n = 8/9*; PAK2 KO, *n = 10/10*; PAK1/2 dKO, *n = 9/9*. Main effects are indicated in the panels. Significant one-way ANOVA and interactions in two-way (RM when applicable) ANOVA were evaluated by Tukey's post hoc test: Insulin-stimulation vs. basal control *** ($p<0.001$); Control vs. PAK2 mKO £ ($p<0.05$); PAK1 KO vs. PAK2 mKO § ($p<0.05$). Data are presented as mean ± S.E.M. with individual data points shown. Paired data points are connected with a straight line.

Figure 7: Lack of PAK2 affects TBC1D4 protein expression and signalling. (A-J) Quantification of phosphorylated (p)Akt S473, pAkt T308, pTBC1D4 T642 and total TBC1D4 and GLUT4 protein expression in insulin-stimulated (60 nM) soleus (A, C, E, G, and I) and extensor digitorum longus (EDL; B, D, F, H, and J) muscle from whole-body PAK1 knockout (KO), muscle-specific PAK2 (m)KO, PAK1/2 double KO (d1/2KO) mice or control littermates. The mice were 10-16 weeks of age. Total protein expression is an average of the paired basal and insulin-stimulated sample. Some of the data points were excluded due to the quality of the immunoblot, so the number of determinations for GLUT4 in soleus muscle: Control, *n = 6*; PAK1 KO, *n = 5*; PAK2 KO, *n = 6*; PAK1/2 dKO, *n = 6*. **(K-L)** Representative blots showing pAkt S473, pAkt T308, pTBC1D4 T642 and total PAK1, PAK2, Akt2, TBC1D4 and GLUT4 protein expression and coomassie staining as a loading control in soleus (K) and EDL (L) muscle. Statistics for phosphorylated proteins were evaluated with a two two-way ANOVAs to test the factors 'PAK1' (PAK1+/- vs. PAK-/-) and 'PAK2' ($PAK2^{fl/fl}$;$MyoD^{+/+}$ vs. $PAK2^{fl/fl}$;$MyoD^{iCre/+}$) in basal and insulin-stimulated samples, respectively, thereby assessing the relative contribution of PAK1 and

PAK2. Differences between genotypes and the effect of insulin stimulation were assessed with a two-way repeated measures (RM) ANOVA to test the factors 'Genotype' (Control vs. PAK1 KO vs. PAK2 mKO vs. 1/m2 dKO) and 'Stimuli' (Basal vs. Insulin). Statistics for total protein expression were evaluated with a two-way ANOVA to test the factors 'PAK1' (PAK1+/- vs. PAK-/-) and 'PAK2' ($PAK2^{fl/fl}$;$MyoD^{+/+}$ vs. $PAK2^{fl/fl}$;$MyoD^{iCre/+}$) thereby assessing the relative contribution of PAK1 and PAK2, respectively. Differences between genotypes were evaluated with a one-way ANOVA. Main effects are indicated in the panels. Significant one-way ANOVA and interactions in two-way (RM when applicable) ANOVA were evaluated by Tukey's post hoc test: Control vs. PAK2 mKO £ ($p<0.05$). Unless otherwise stated previously in the figure legend, the number of determinations in each group: Control, *n = 9/10* (soleus/EDL); PAK1 KO, *n = 8/9*; PAK2 KO, *n = 10/9*; PAK1/2 dKO, *n = 9/9*. Data are presented as mean ± S.E.M. with individual data points shown. Paired data points are connected with a straight line. A.U., arbitrary units.

Supplementary figures

Figure S1: (A-B) Insulin-stimulated (Chow: 0.5 U kg^{-1} body weight; HFD: 60% of insulin administered to chow-fed mice) 2-Deoxyglucose (2DG) clearance in gastrocnemius (Gast), quadriceps (Quad), triceps brachii (Triceps) and soleus muscle from chow- (A) and 60E% high-fat diet (HFD)-fed (B) PAK1 knockout (KO) mice or control littermates. The number of mice in each group: Chow-Saline, *n = 12/4* (Control/PAK1 KO); Chow-Insulin, *n = 12/6*; HFD-Saline, *n = 6/6*; HFD-Insulin, *n = 10/11*. Statistics were evaluated with a two-way ANOVA for each of the muscles. **(C)** Plasma [^{3}H] counts 10 minutes after retro-orbital (r.o.) administration of a bolus of saline containing [^{3}H]-labelled 2DG ([^{3}H]-2DG) with or without insulin. Statistics were evaluated with two two-way ANOVAs to test the factors 'stimuli' (basal vs. insulin) and 'genotype' (control vs.

PAK1 KO) in chow-fed and HFD-fed mice, respectively. **(D)** Body composition (FM: Fat mass; LBM: Lean body mass; BW: Body weight) in gram in HFD-fed PAK1 KO mice (*n = 17*) or control littermates (*n = 14*). Body composition was assessed in week 18-19 of the diet intervention. The mice were 24-34 weeks of age. Statistics were evaluated with a Student's t-test. **(E)** Energy intake in HFD-fed PAK1 KO mice (*n = 8*) or control littermates (*n = 8*). Energy intake was monitored in a separate cohort of mice. Statistics were evaluated with a Student's t-test. **(F)** Blood glucose levels during a glucose tolerance test (GTT) in HFD-fed PAK1 KO mice (*n = 17*) or control littermates (*n = 13*). Glucose tolerance was assessed in week 14 of the diet intervention. The mice were 20-30 weeks of age. Statistics were evaluated with a two-way repeated measures (RM) ANOVA. **(G)** Incremental Area Under the Curve (AUC) for blood glucose levels during the GTT in panel F. Statistics were evaluated with a Student's t-test. **(H)** Plasma insulin values during a GTT in HFD-fed PAK1 KO mice (*n = 16*) or control littermates (*n = 11*). The plasma insulin response to glucose administration was measured in week 16 of the diet intervention. The mice were 22-32 weeks of age. Statistics were evaluated with a two-way RM ANOVA. **(I)** Homeostatic Model Assessment of Insulin Resistance (HOMA-IR) in HFD-fed PAK1 KO mice (*n = 16*) or control littermates (*n = 11*). Statistics were evaluated with a Student's t-test. Main effects are indicated in the panels. Data are presented as mean ± S.E.M. or when applicable mean ± S.E.M. with individual data points shown. Paired data points are connected with a straight line.

Figure S2: (A-B) Body weight of female (A) and male (B) whole-body PAK1 knockout (KO), muscle-specific PAK2 (m)KO, PAK1/2 double KO (d1/2KO) mice or control littermates. **(C-D)** Body composition (FM: Fat mass; LBM: Lean body mass) in gram in female (C) and male (D) PAK1 KO, PAK2 mKO, 1/m2 dKO or control littermates. **(E-G)** Body composition (FM: Fat mass; LBM: Lean body mass) in percentage in both sexes combined (E) and in female (F) and male (G) PAK1 KO, PAK2 mKO, 1/m2 dKO or control littermates. The number of mice in each group:

Control, *n = 9/11* (female/male); PAK1 KO, *n = 8/10*; PAK2 mKO, *n = 12/9*; 1/m2 dKO, *n = 9/14*. Statistics were evaluated with a two-way ANOVA to test the factors 'PAK1' (PAK1+/- vs. PAK-/-) and 'PAK2' ($PAK2^{fl/fl}$;$MyoD^{+/+}$ vs. $PAK2^{fl/fl}$;$MyoD^{iCre/+}$) thereby assessing the relative contribution of PAK1 and PAK2, respectively. Differences between genotypes were evaluated with a one-way ANOVA. Main effects are indicated in the panels. Significant one-way ANOVA and interactions in two-way ANOVA were evaluated by Tukey's post hoc test: Control vs. 1/m2 dKO †/†† ($p<0.05/0.01$); PAK1 KO vs. PAK2 mKO § ($p<0.05$); PAK1 KO vs. 1/m2 dKO ‡/‡‡/‡‡‡ ($p<0.05/0.01/0.001$); PAK2 mKO vs. 1/m2 dKO ($)/$$ ($p<0.1/0.01$). Data are presented as mean ± S.E.M. with individual data points shown.

Figure S3: (A-F) Oxygen uptake (VO_2), respiratory exchange ratio (RER), and activity (beam breaks) in female (A,C, and E) and male (B,D, and F) whole-body PAK1 knockout (KO), muscle-specific PAK2 (m)KO, PAK1/2 double KO (d1/2KO) mice or control littermates during the light and dark period recorded over a period of 72 hours in calorimetric chambers. On day 2, mice fasted during the dark period and then refed on day 3. **(G-I)** Total energy intake on day 1 and day 3 in both sexes combined (G) and in female (H) and male (I) whole-body PAK1 KO, PAK2 mKO, 1/m2 dKO mice or control littermates recorded over a period of 72 hours in calorimetric chambers. **(J-K)** Energy intake in female (J) and male (K) whole-body PAK1 KO, Pak2 mKO, 1/m2 dKO mice or control littermates during the light and dark period recorded over a period of 72 hours in calorimetric chambers. On day 2, mice fasted during the dark period and were then refed on day 3. The number of mice in each group: Control, *n = 5/3* (female/male; for energy intake, *n = 4/3*); PAK1 KO, *n = 6/5*; PAK2 mKO, *n = 6/5*; 1/m2 dKO, *n = 6/7*. **(A-F+J-K)** Statistics were evaluated with two two-way ANOVAs to test the factors 'PAK1' (PAK1+/- vs. PAK-/-) and 'PAK2' ($PAK2^{fl/fl}$;$MyoD^{+/+}$ vs. $PAK2^{fl/fl}$;$MyoD^{iCre/+}$) in the light and dark period of day 1, respectively. Statistics for day 2 and 3 were evaluated similarly thereby assessing the relative contribution of

PAK1 and PAK2. Differences between genotypes and the effect of the light and the dark period were assessed with three two-way repeated measures (RM) ANOVA to test the factors 'Genotype' (Control vs. PAK1 KO vs. PAK2 mKO vs. 1/m2 dKO) and 'Period' (Light vs. Dark) at day 1, 2 and 3, respectively. **(G-I)** Statistics were evaluated with two two-way ANOVAs to test the factors 'PAK1' (PAK1+/- vs. PAK-/-) and 'PAK2' ($PAK2^{fl/fl}$;$MyoD^{+/+}$ vs. $PAK2^{fl/fl}$;$MyoD^{iCre/+}$) at day 1 and day 2, respectively. Differences between genotypes and the day were assessed with one two-way repeated measures (RM) ANOVA to test the factors 'Genotype' (Control vs. PAK1 KO vs. PAK2 mKO vs. 1/m2 dKO) and 'Day' (Day 1 vs. Day 3). Main effects are indicated in the panels. Significant one-way ANOVA and interactions in two-way (RM when applicable) ANOVA were evaluated by Tukey's post hoc test: Light vs. dark period */**/*** ($p<0.05/0.01/0.001$); Day 1 vs. Day 3 €€/€€€ ($p<0.01/0.001$); Control vs. PAK1 KO ¤¤ ($p<0.01$); Control vs. 1/m2 dKO † ($p<0.05$); PAK1 KO vs. PAK2 mKO §/§§ ($p<0.05/0.01$); PAK1 KO vs. 1/m2 dKO ‡/‡‡/‡‡‡ ($p<0.05/0.01/0.001$). Data are presented as mean ± S.E.M. with individual data points shown.

Figure S4: (A-B) Blood glucose concentration in the fed state (8 a.m.) in female (A) and male (B) whole-body PAK1 knockout (KO), muscle-specific PAK2 (m)KO, PAK1/2 double KO (d1/2KO) mice or control littermates. The number of mice in each group: Control, *n = 9/11* (female/male); PAK1 KO, *n = 8/10*; PAK2 mKO, *n = 12/9*; 1/m2 dKO, *n = 9/14*. Statistics were evaluated with a two-way ANOVA to test the factors 'PAK1' (PAK1+/- vs. PAK-/-) and 'PAK2' ($PAK2^{fl/fl}$;$MyoD^{+/+}$ vs. $PAK2^{fl/fl}$;$MyoD^{iCre/+}$) thereby assessing the relative contribution of PAK1 and PAK2, respectively. Differences between genotypes were evaluated with a one-way ANOVA. **(C-D)** Blood glucose levels during a glucose tolerance test (GTT) in female (C) and male (D) PAK1 KO, PAK2 mKO, 1/m2 dKO mice or control littermates. The number of mice in each group: Control, *n = 8/11* (female/male); PAK1 KO, *n = 8/10*; PAK2 mKO, *n = 10/9*; 1/m2 dKO, *n = 8/13*. Statistics were evaluated with six two-way ANOVAs to test the factors 'PAK1' (PAK1+/- vs. PAK-/-) and 'PAK2'

(PAK2$^{fl/fl}$;MyoD$^{+/+}$ vs. PAK2$^{fl/fl}$;MyoD$^{iCre/+}$) at time point 0, 15, 30, 60, 90 and 120, respectively, thereby assessing the relative contribution of PAK1 and PAK2. Differences between genotypes and the effect of glucose administration were assessed with a two-way repeated measures (RM) ANOVA to test the factors 'Genotype' (Control vs. PAK1 KO vs. PAK2 mKO vs. 1/m2 dKO) and 'Time' (0 vs. 15 vs. 30 vs. 60 vs. 90 vs. 120). **(E-F)** Incremental Area Under the Curve (AUC) for blood glucose levels for females (E) and male (F) mice during the GTT in panel C-D. Statistics were evaluated with a two-way ANOVA to test the factors 'PAK1' (PAK1+/- vs. PAK-/-) and 'PAK2' (PAK2$^{fl/fl}$;MyoD$^{+/+}$ vs. PAK2$^{fl/fl}$;MyoD$^{iCre/+}$) thereby assessing the relative contribution of PAK1 and PAK2, respectively. Differences between genotypes were evaluated with a one-way ANOVA. **(G-H)** Plasma insulin values during a GTT in female (G) and male (F) PAK1 KO, PAK2 mKO, 1/m2 dKO mice or control littermates. The number of mice in each group: Control, *n = 9/10* (female/male); PAK1 KO, *n = 8/9*; PAK2 mKO, *n = 10/9*; 1/m2 dKO, *n = 9/13*. Statistics were evaluated with two two-way ANOVAs to test the factors 'PAK1' (PAK1+/- vs. PAK-/-) and 'PAK2' (PAK2$^{fl/fl}$;MyoD$^{+/+}$ vs. PAK2$^{fl/fl}$;MyoD$^{iCre/+}$) at time point 0 and 20, respectively, thereby assessing the relative contribution of PAK1 and PAK2. Differences between genotypes and the effect of glucose administration were assessed with a two-way RM ANOVA to test the factors 'Genotype' (Control vs. PAK1 KO vs. PAK2 mKO vs. 1/m2 dKO) and 'Time' (0 vs. 20). Main effects are indicated in the panels. Significant one-way ANOVA and interactions in two-way (RM when applicable) ANOVA were evaluated by Tukey's post hoc test: Effect of glucose administration vs. time point 0' */*** ($p<0.05/0.001$); Control vs. PAK2 mKO £ ($p<0.05$); PAK1 KO vs. PAK2 mKO §§ ($p<0.01$); PAK2 mKO vs. 1/m2 dKO $ ($p<0.05$). Data are presented as mean ± S.E.M. or when applicable mean ± S.E.M. with individual data points shown. Paired data points are connected with a straight line.

Figure S5: (A-B) Homeostatic Model Assessment of Insulin Resistance (HOMA-IR) in female (A) and male (B) whole-body PAK1 knockout (KO), muscle-specific PAK2 (m)KO, PAK1/2 double KO (d1/2KO) mice or control littermates. The number of mice in each group: Control, *n = 9/11* (female/male); PAK1 KO, *n = 8/10*; PAK2 mKO, *n = 10/9*; 1/m2 dKO, *n = 9/13*. Statistics were evaluated with a two-way ANOVA to test the factors 'PAK1' (PAK1+/- vs. PAK-/-) and 'PAK2' ($PAK2^{fl/fl}$;$MyoD^{+/+}$ vs. $PAK2^{fl/fl}$;$MyoD^{iCre/+}$) thereby assessing the relative contribution of PAK1 and PAK2, respectively. Genotype differences were evaluated with a one-way ANOVA. **(C-E)** Basal blood glucose concentration (fasted state) immediately before an insulin tolerance test (ITT) in both sexes combined (C) and in female (D) and male (E) PAK1 KO, PAK2 mKO, 1/m2 dKO mice and control littermates. The number of mice in each group: Control, *n = 9/10* (female/male); PAK1 KO, *n = 6/9*; PAK2 mKO, *n = 10/8*; 1/m2 dKO, *n = 8/13*. Statistics were evaluated with a two-way ANOVA to test the factors 'PAK1' (PAK1+/- vs. PAK-/-) and 'PAK2' ($PAK2^{fl/fl}$;$MyoD^{+/+}$ vs. $PAK2^{fl/fl}$;$MyoD^{iCre/+}$) thereby assessing the relative contribution of PAK1 and PAK2, respectively. Differences between genotypes were evaluated with a one-way ANOVA. **(F-G)** Blood glucose levels related to basal concentration during an ITT in female (F) and male (G) PAK1 KO, PAK2 mKO, 1/m2 dKO mice or control littermates. The number of mice in each group: Control, *n = 9/10* (female/male); PAK1 KO, *n = 6/9*; PAK2 mKO, *n = 10/8*; 1/m2 dKO, *n = 8/13*. For two female control mice and four female PAK2 mKO mice, the ITT had to be stopped before the 120'-time point due to hypoglycemia (blood glucose <1.2 mM), and thus blood glucose was not determined for these mice for the last couple of time points. Statistics were evaluated with five two-way ANOVAs to test the factors 'PAK1' (PAK1+/- vs. PAK-/-) and 'PAK2' ($PAK2^{fl/fl}$;$MyoD^{+/+}$ vs. $PAK2^{fl/fl}$;$MyoD^{iCre/+}$) at time point 15, 30, 60, 90 and 120, respectively, thereby assessing the relative contribution of PAK1 and PAK2. Differences between genotypes and the effect of insulin administration were assessed with a two-way repeated measures (RM) ANOVA (mixed-effects

model analysis for female mice) to test the factors 'Genotype' (Control vs. PAK1 KO vs. PAK2 mKO vs. 1/m2 dKO) and 'Time' (0 vs. 15 vs. 30 vs. 60 vs. 90 vs. 120). Main effects are indicated in the panels. Significant one-way ANOVA and interactions in two-way (RM when applicable) ANOVA were evaluated by Tukey's post hoc test: Effect of insulin administration vs. time point 0' **/*** ($p<0.01/0.001$); Control vs. PAK1 KO ¤/¤¤ ($p<0.05/0.01$); Control vs. PAK2 mKO (£)££ ($p<0.1/0.01$); Control vs. 1/m2 dKO ††† ($p<0.001$); PAK1 KO vs. 1/m2 dKO ‡ ($p<0.05$); PAK2 mKO vs. 1/m2 dKO $ ($p<0.05$). Data are presented as mean ± S.E.M. or when applicable mean ± S.E.M. with individual data points shown.

Figure S6: (A-D) Δ-phosphorylated (p)-Akt S473 and ΔpAkt T308 in insulin-stimulated (60 nM) soleus (A and C) and extensor digitorum longus (EDL; B and D) muscle from whole-body PAK1 knockout (KO), muscle-specific PAK2 (m)KO, PAK1/2 double KO (d1/2KO) mice or control littermates from Fig. 7A-D. **(E-F)** Quantification of total Akt2 protein expression in soleus (E) and EDL (F) muscle from whole-body PAK1 KO, PAK2 mKO, 1/m2 dKO mice or control littermates. Total protein expression is an average of the paired basal and insulin-stimulated sample. **(G-H)** ΔpTBC1D4 T642 in insulin-stimulated (60 nM) soleus (G) and EDL (H) muscle from whole-body PAK1 KO, PAK2 mKO, 1/m2 dKO mice or control littermates from Fig. 7G-H. Statistics were evaluated with a two-way ANOVA to test the factors 'PAK1' (PAK1+/- vs. PAK-/-) and 'PAK2' ($PAK2^{fl/fl}$;$MyoD^{+/+}$ vs. $PAK2^{fl/fl}$;$MyoD^{iCre/+}$) thereby assessing the relative contribution of PAK1 and PAK2, respectively. Differences between genotypes were evaluated with a one-way ANOVA. The number of determinations in each group: Control, *n = 9/10* (soleus/EDL); PAK1 KO, *n = 8/9*; PAK2 KO, *n = 10/9*; PAK1/2 dKO, *n = 9/9*. Significant one-way ANOVA was evaluated by Tukey's post hoc test: Control vs. PAK2 mKO £ ($p<0.05$). Data are presented as mean ± S.E.M. with individual data points shown. A.U., arbitrary units.

Figure 1

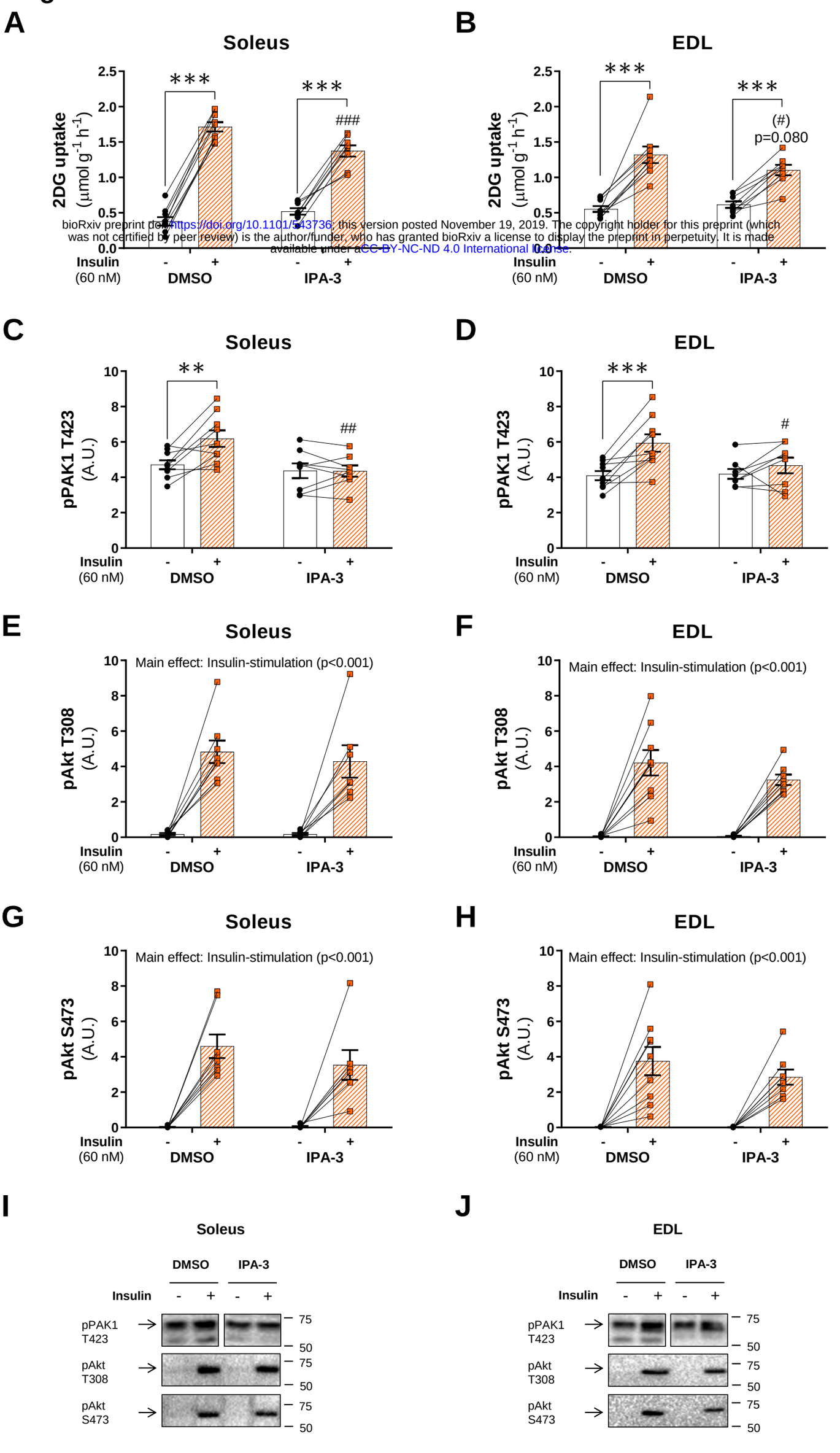

Figure 2

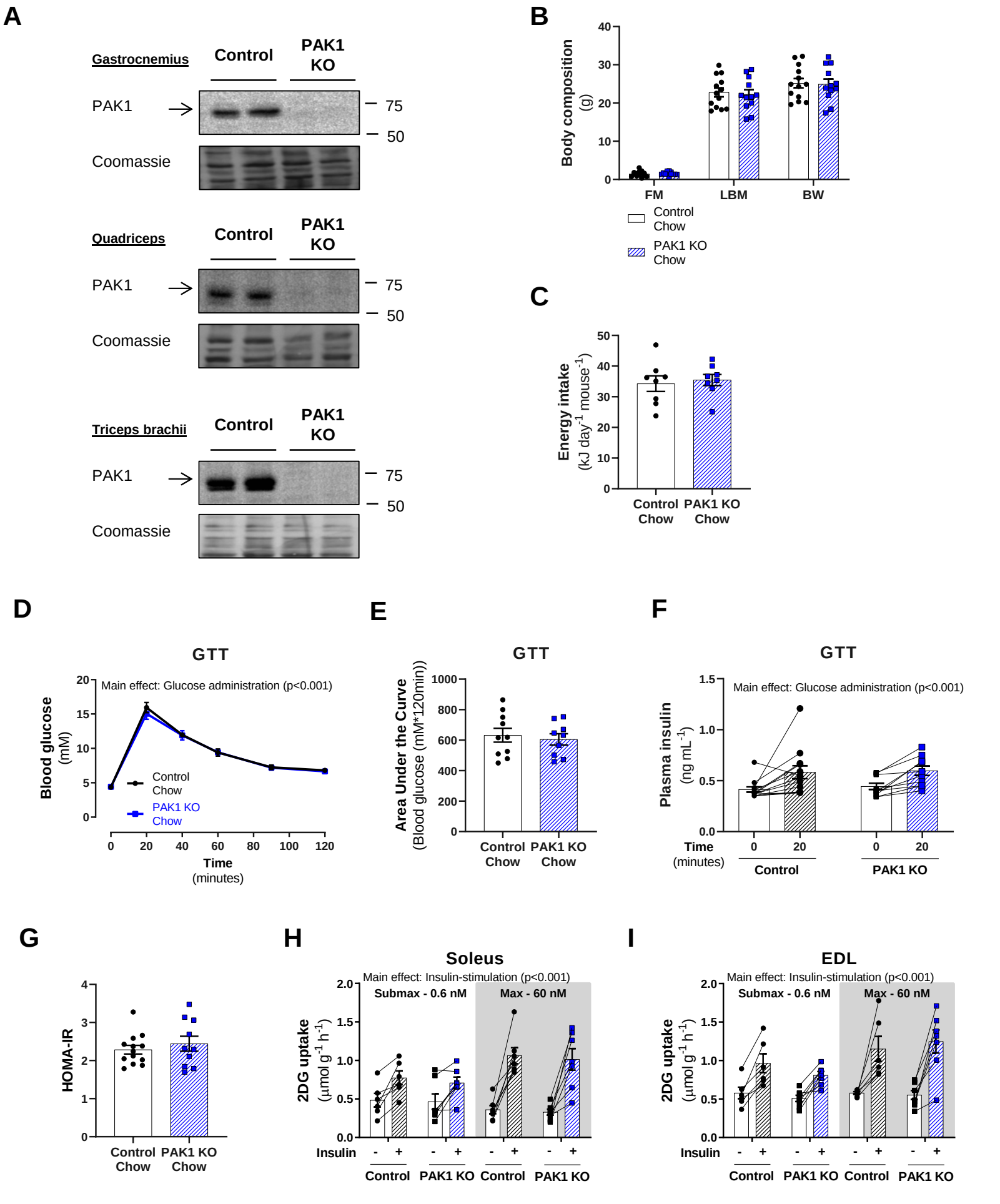
A
Gastrocnemius
Control
PAK1 KO
PAK1
Coomassie
75
50
Quadriceps
Triceps brachii
B
Body composition (g)
FM
LBM
BW
Control Chow
PAK1 KO Chow
C
Energy intake (kJ day-1 mouse-1)
D
GTT
Main effect: Glucose administration (p<0.001)
Blood glucose (mM)
Time (minutes)
E
Area Under the Curve (Blood glucose (mM*120min))
F
Plasma insulin (ng mL-1)
Time (minutes)
G
HOMA-IR
H
Soleus
Main effect: Insulin-stimulation (p<0.001)
Submax - 0.6 nM
Max - 60 nM
2DG uptake (µmol g-1 h-1)
Insulin
I
EDL

Figure 3

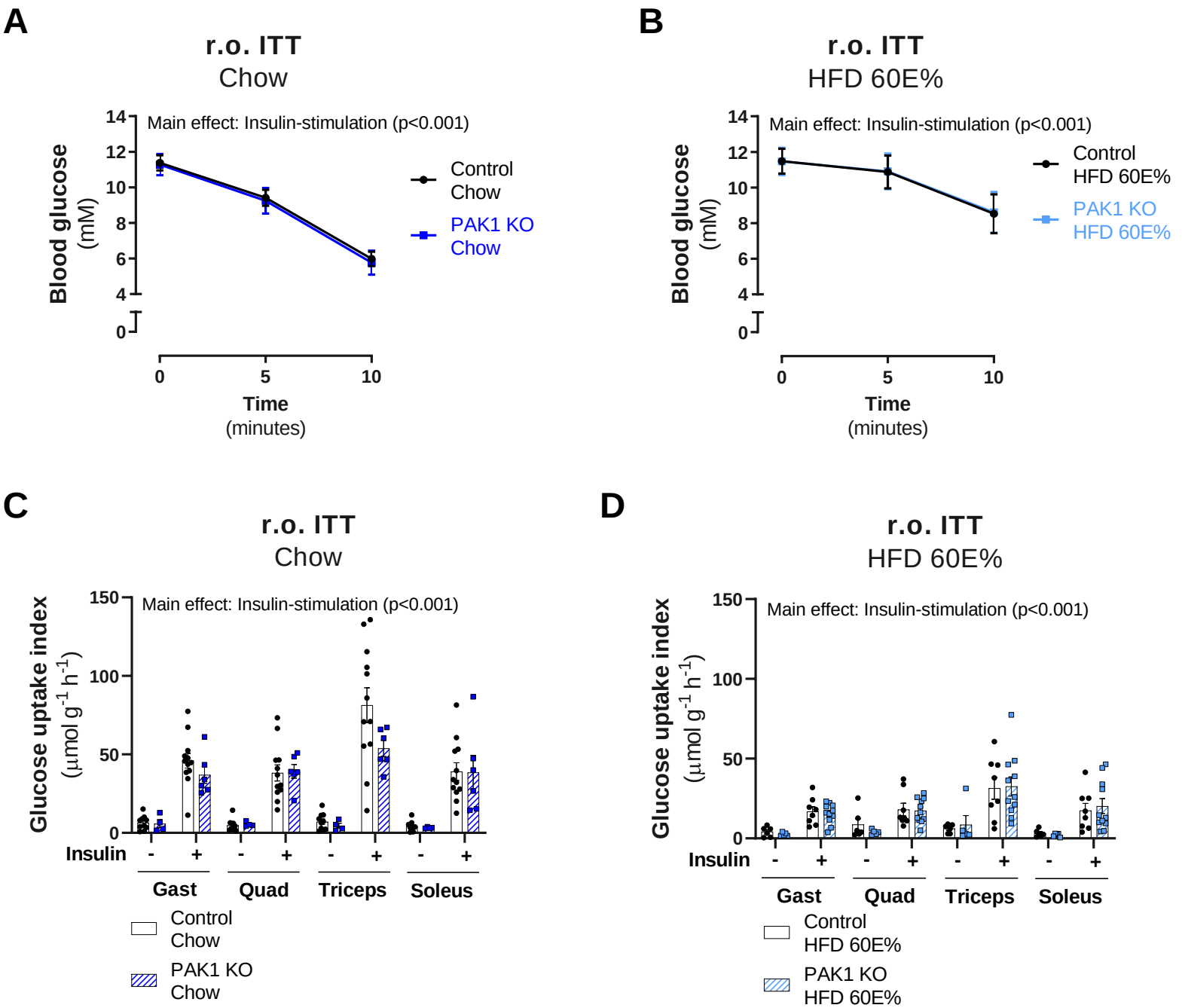
A
r.o. ITT
Chow
Main effect: Insulin-stimulation (p<0.001)
Blood glucose (mM)
Time (minutes)
Control Chow
PAK1 KO Chow
B
r.o. ITT
HFD 60E%
Main effect: Insulin-stimulation (p<0.001)
Blood glucose (mM)
Time (minutes)
Control HFD 60E%
PAK1 KO HFD 60E%
C
r.o. ITT
Chow
Main effect: Insulin-stimulation (p<0.001)
Glucose uptake index (µmol g-1 h-1)
Insulin
Gast
Quad
Triceps
Soleus
Control Chow
PAK1 KO Chow
D
r.o. ITT
HFD 60E%
Main effect: Insulin-stimulation (p<0.001)
Glucose uptake index (µmol g-1 h-1)
Insulin
Gast
Quad
Triceps
Soleus
Control HFD 60E%
PAK1 KO HFD 60E%

Figure 4

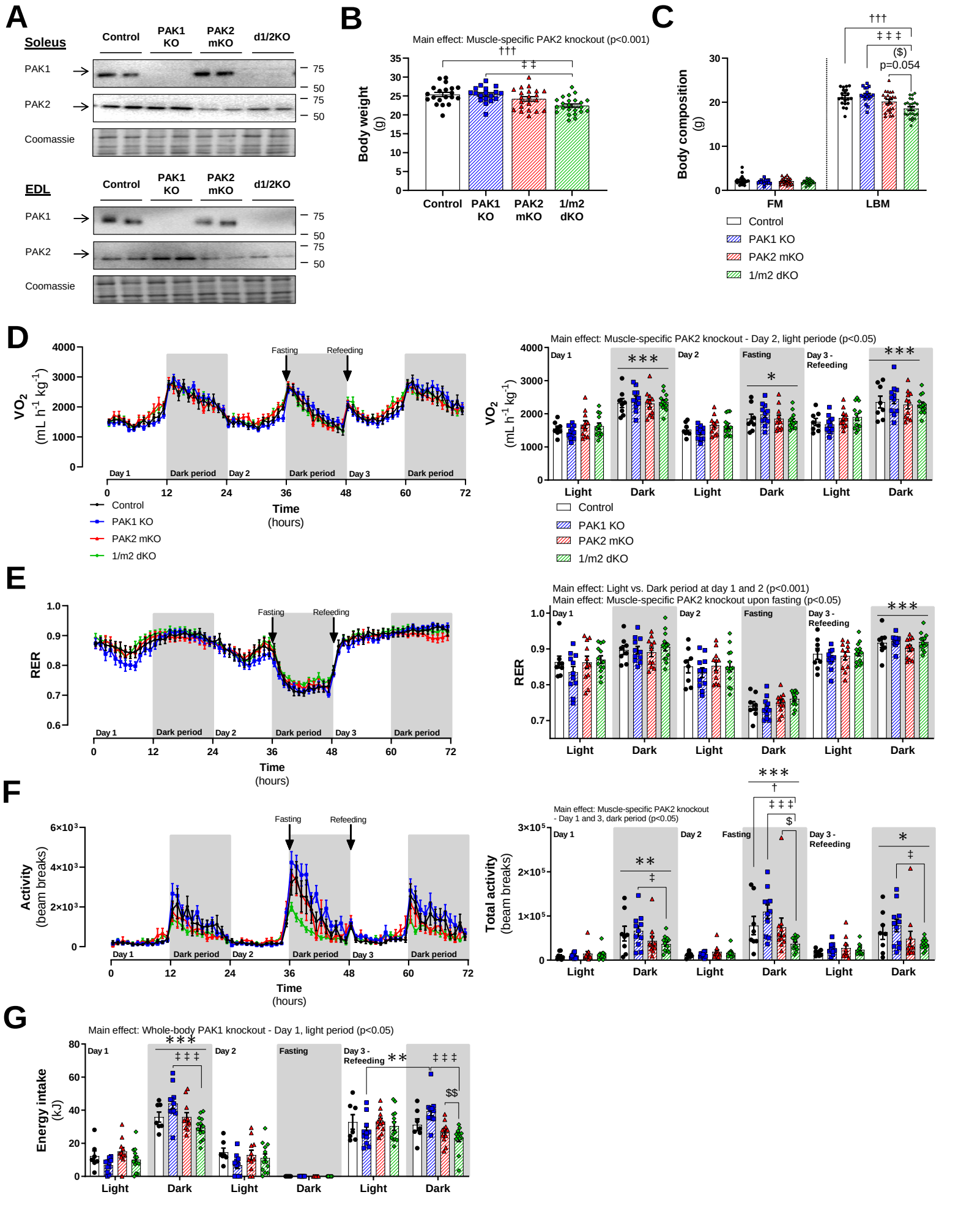
A
Soleus
Control
PAK1 KO
PAK2 mKO
d1/2KO
PAK1
PAK2
Coomassie
75
50
75
50
EDL
Control
PAK1 KO
PAK2 mKO
d1/2KO
PAK1
PAK2
Coomassie
75
50
75
50
B
Main effect: Muscle-specific PAK2 knockout (p<0.001)
Body weight (g)
Control
PAK1 KO
PAK2 mKO
1/m2 dKO
C
Body composition (g)
FM
LBM
p=0.054
Control
PAK1 KO
PAK2 mKO
1/m2 dKO
D
VO2 (mL h-1 kg-1)
Fasting
Refeeding
Day 1
Dark period
Day 2
Dark period
Day 3
Dark period
Time (hours)
Control
PAK1 KO
PAK2 mKO
1/m2 dKO
Main effect: Muscle-specific PAK2 knockout - Day 2, light periode (p<0.05)
Day 1
Day 2
Fasting
Day 3 - Refeeding
Light
Dark
E
RER
Fasting
Refeeding
Time (hours)
Main effect: Light vs. Dark period at day 1 and 2 (p<0.001)
Main effect: Muscle-specific PAK2 knockout upon fasting (p<0.05)
F
Activity (beam breaks)
Time (hours)
Main effect: Muscle-specific PAK2 knockout - Day 1 and 3, dark period (p<0.05)
Total activity (beam breaks)
G
Main effect: Whole-body PAK1 knockout - Day 1, light period (p<0.05)
Energy intake (kJ)

Figure 5

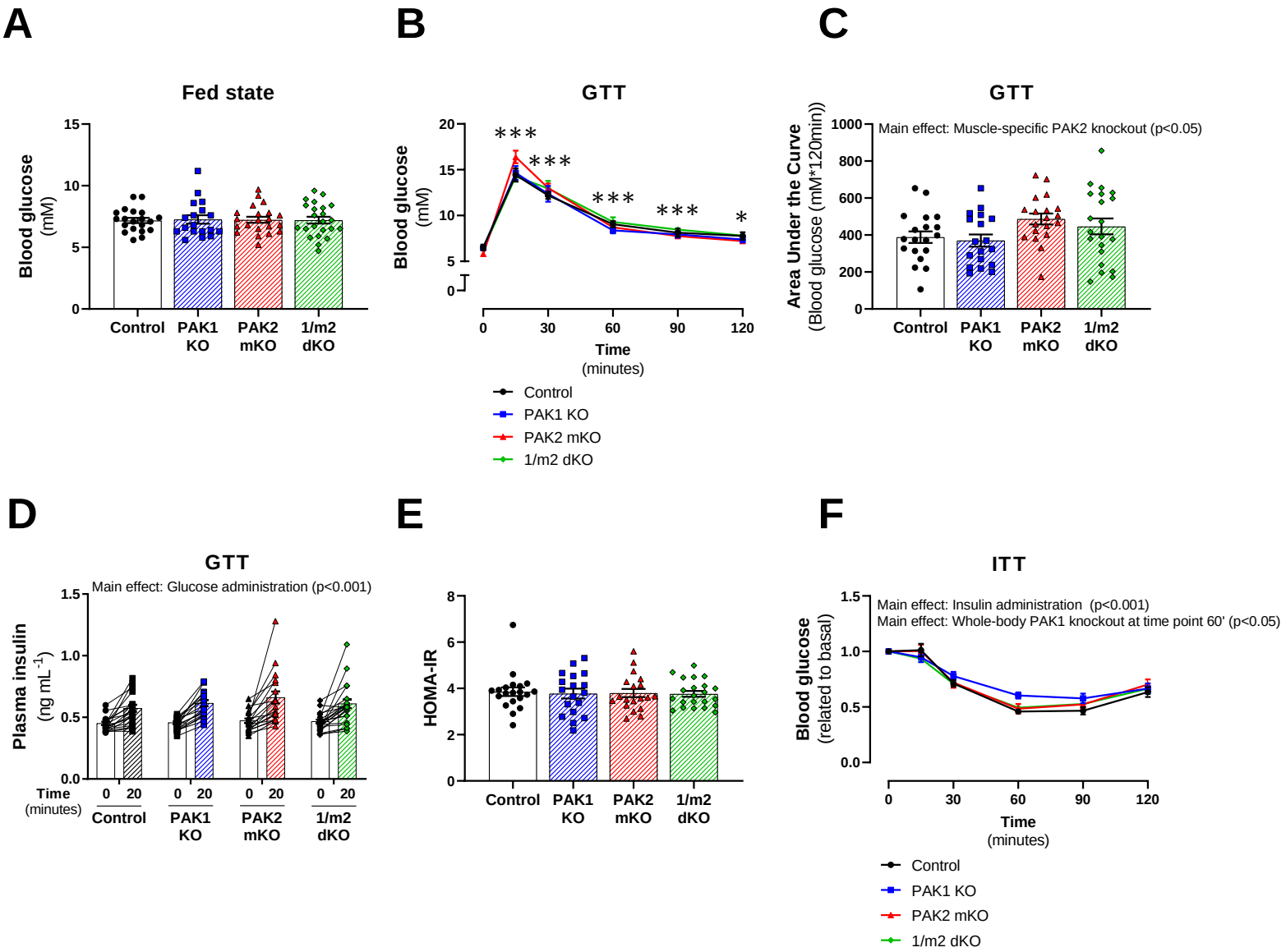
A
Fed state
Blood glucose (mM)
Control
PAK1 KO
PAK2 mKO
1/m2 dKO
B
GTT
Blood glucose (mM)
***
***
***
***
*
Time (minutes)
Control
PAK1 KO
PAK2 mKO
1/m2 dKO
C
GTT
Area Under the Curve (Blood glucose (mM*120min))
Main effect: Muscle-specific PAK2 knockout (p<0.05)
D
GTT
Main effect: Glucose administration (p<0.001)
Plasma insulin (ng mL-1)
Time (minutes)
E
HOMA-IR
F
ITT
Main effect: Insulin administration (p<0.001)
Main effect: Whole-body PAK1 knockout at time point 60' (p<0.05)
Blood glucose (related to basal)
Time (minutes)

Figure 6

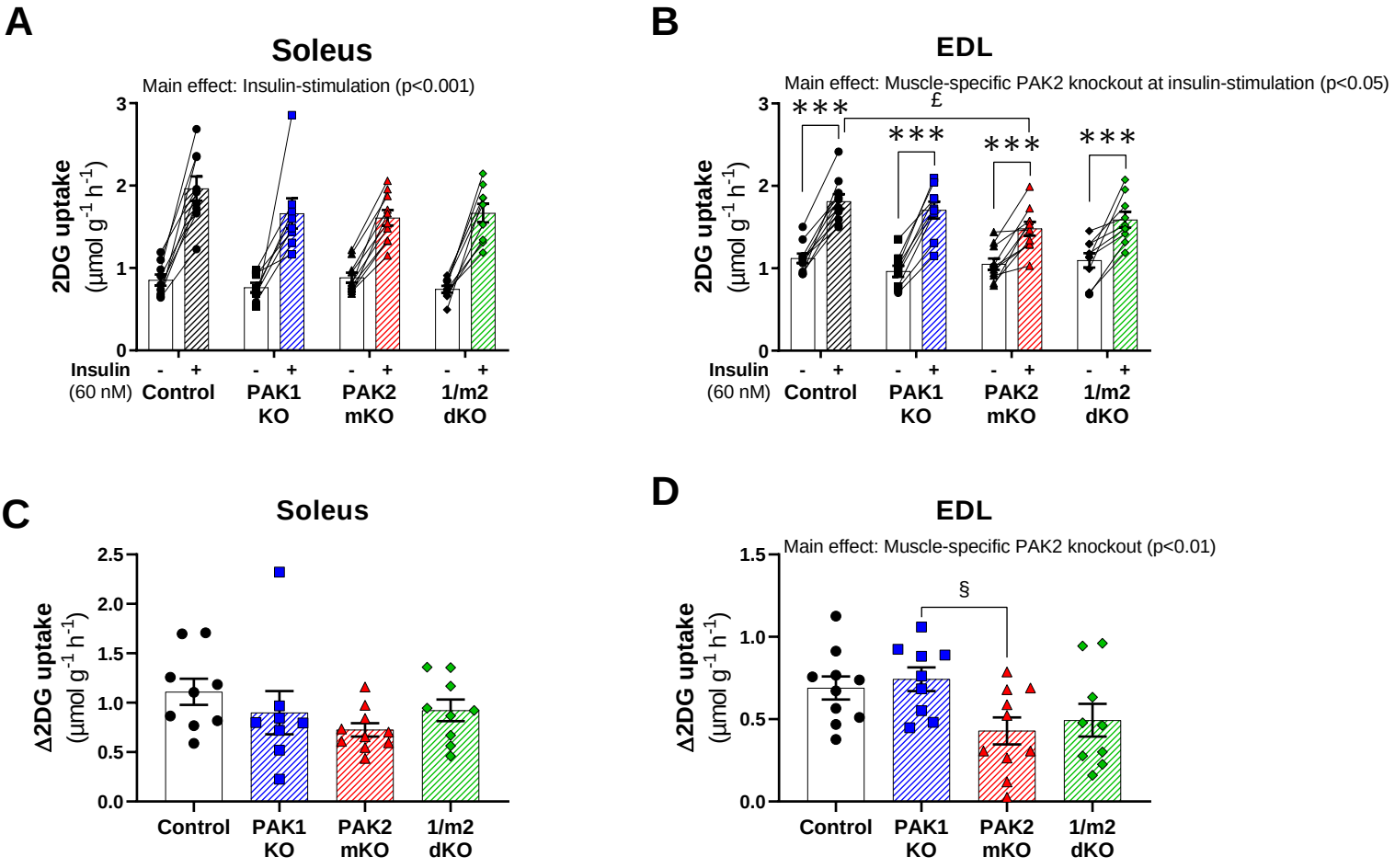
A
Soleus
Main effect: Insulin-stimulation (p<0.001)
2DG uptake
(µmol g-1 h-1)
Insulin
(60 nM)
Control
PAK1 KO
PAK2 mKO
1/m2 dKO
B
EDL
Main effect: Muscle-specific PAK2 knockout at insulin-stimulation (p<0.05)
***
£
C
Soleus
Δ2DG uptake
(µmol g-1 h-1)
D
EDL
Main effect: Muscle-specific PAK2 knockout (p<0.01)
§

Figure 7

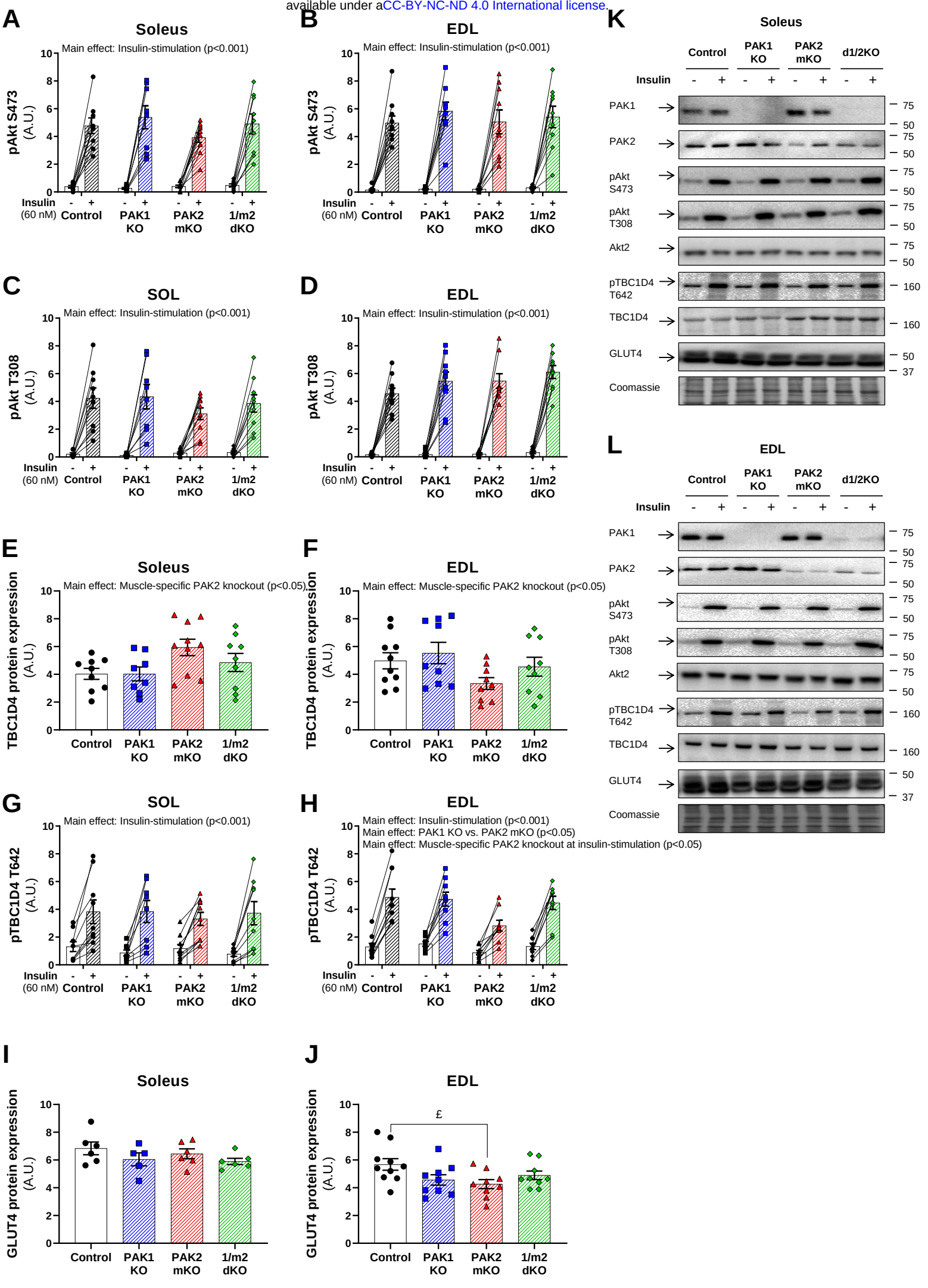

Figure S1

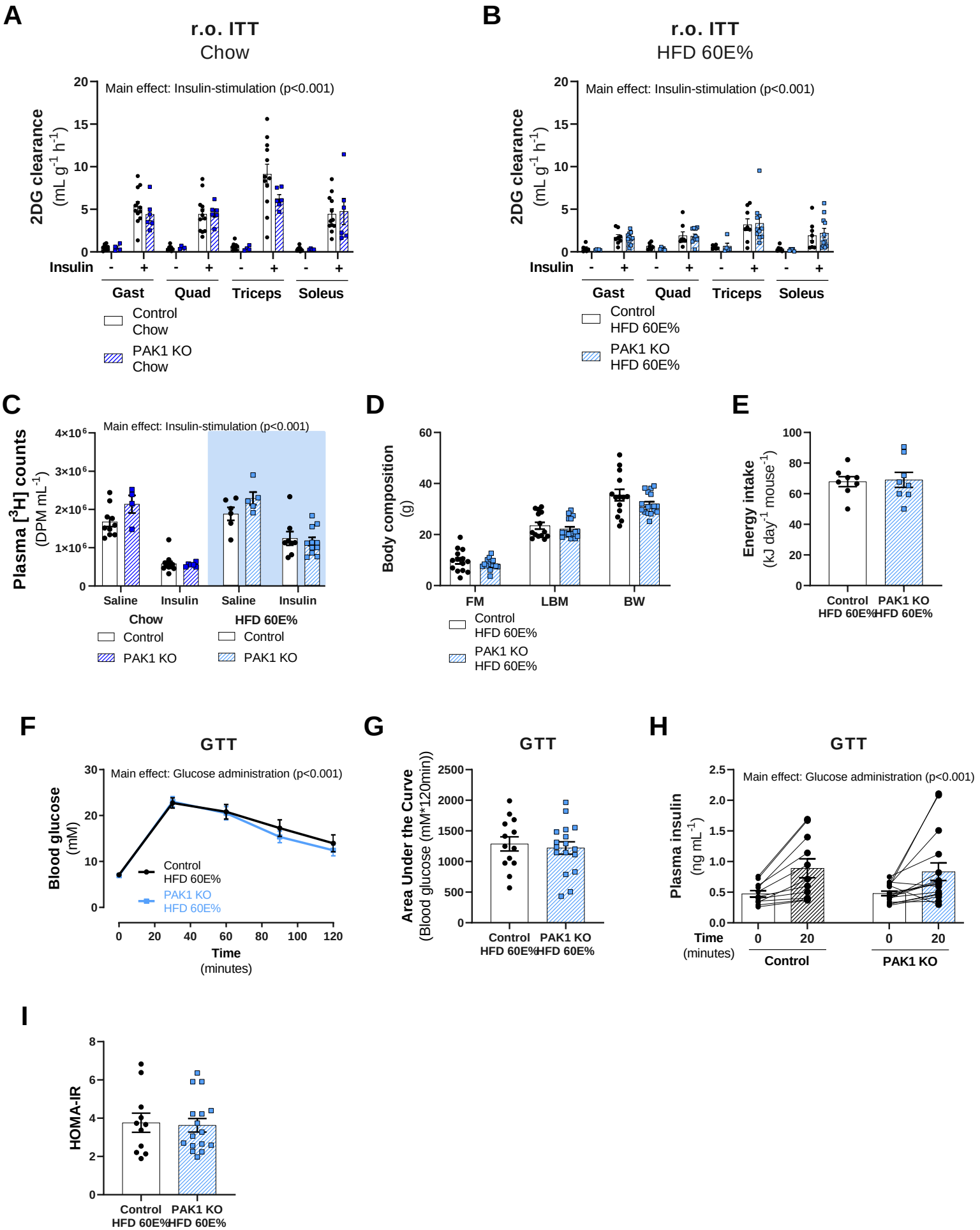
A
r.o. ITT
Chow
Main effect: Insulin-stimulation (p<0.001)
2DG clearance
(mL g-1 h-1)
Insulin
Gast
Quad
Triceps
Soleus
Control
Chow
PAK1 KO
Chow
B
r.o. ITT
HFD 60E%
Main effect: Insulin-stimulation (p<0.001)
2DG clearance
(mL g-1 h-1)
Insulin
Gast
Quad
Triceps
Soleus
Control
HFD 60E%
PAK1 KO
HFD 60E%
C
Main effect: Insulin-stimulation (p<0.001)
Plasma [3H] counts
(DPM mL-1)
Saline
Insulin
Saline
Insulin
Chow
HFD 60E%
Control
PAK1 KO
Control
PAK1 KO
D
Body composition
(g)
FM
LBM
BW
Control
HFD 60E%
PAK1 KO
HFD 60E%
E
Energy intake
(kJ day-1 mouse-1)
Control
HFD 60E%
PAK1 KO
HFD 60E%
F
GTT
Main effect: Glucose administration (p<0.001)
Blood glucose
(mM)
Control
HFD 60E%
PAK1 KO
HFD 60E%
Time
(minutes)
G
GTT
Area Under the Curve
(Blood glucose (mM*120min))
Control
HFD 60E%
PAK1 KO
HFD 60E%
H
GTT
Main effect: Glucose administration (p<0.001)
Plasma insulin
(ng mL-1)
Time
(minutes)
Control
PAK1 KO
I
HOMA-IR
Control
HFD 60E%
PAK1 KO
HFD 60E%

Figure S2

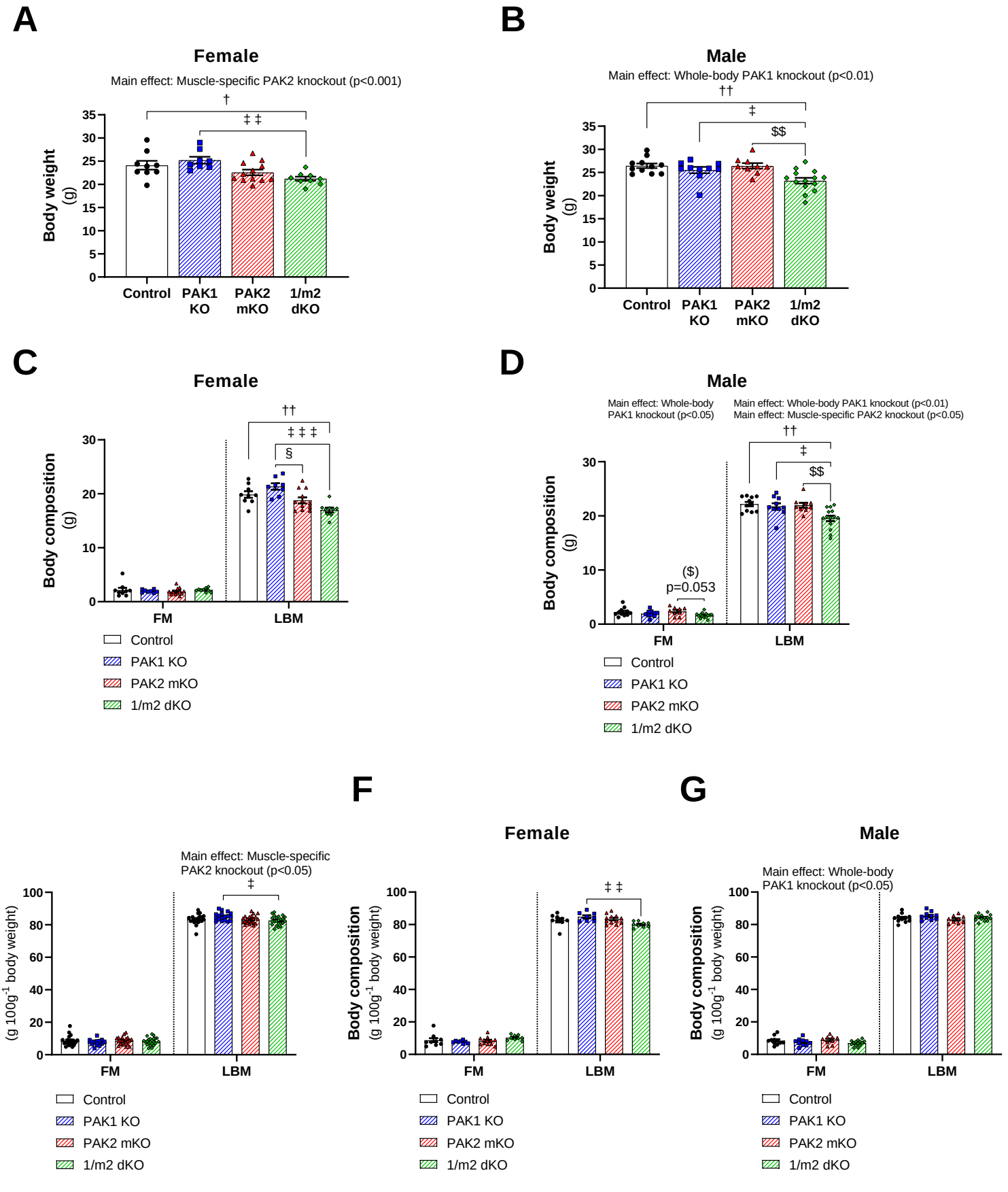
A
Female
Main effect: Muscle-specific PAK2 knockout (p<0.001)
Body weight (g)
Control
PAK1 KO
PAK2 mKO
1/m2 dKO
B
Male
Main effect: Whole-body PAK1 knockout (p<0.01)
C
Female
Body composition (g)
FM
LBM
D
Male
Main effect: Whole-body PAK1 knockout (p<0.05)
Main effect: Whole-body PAK1 knockout (p<0.01)
Main effect: Muscle-specific PAK2 knockout (p<0.05)
($) p=0.053
E
Main effect: Muscle-specific PAK2 knockout (p<0.05)
Body composition (g 100g-1 body weight)
F
Female
G
Male
Main effect: Whole-body PAK1 knockout (p<0.05)

Figure S3

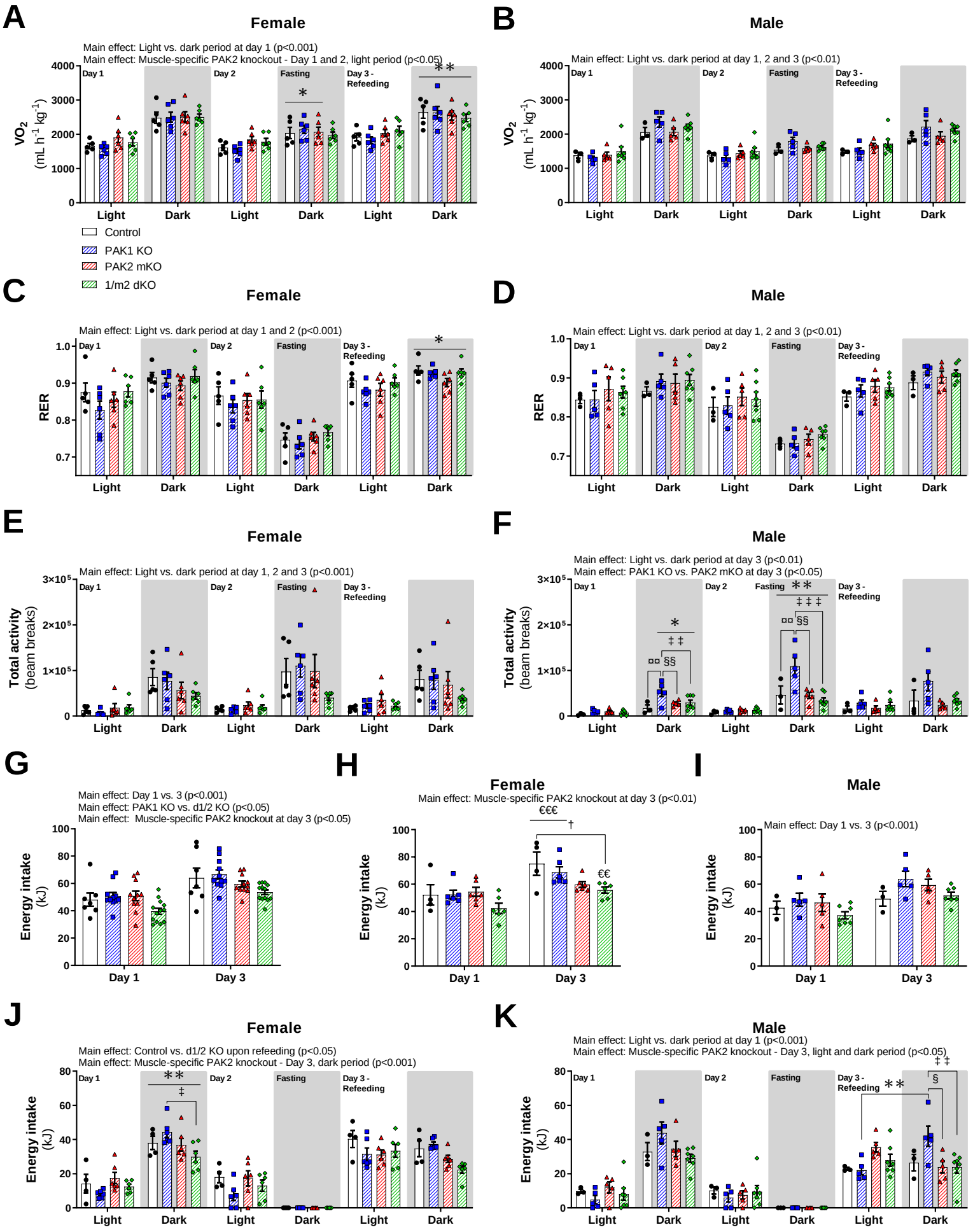
A
Female
Main effect: Light vs. dark period at day 1 (p<0.001)
Main effect: Muscle-specific PAK2 knockout - Day 1 and 2, light period (p<0.05)
VO2 (mL h-1 kg-1)
Day 1
Day 2
Fasting
Day 3 - Refeeding
Light
Dark
Control
PAK1 KO
PAK2 mKO
1/m2 dKO
B
Male
Main effect: Light vs. dark period at day 1, 2 and 3 (p<0.01)
C
Female
Main effect: Light vs. dark period at day 1 and 2 (p<0.001)
RER
D
Male
Main effect: Light vs. dark period at day 1, 2 and 3 (p<0.01)
E
Female
Main effect: Light vs. dark period at day 1, 2 and 3 (p<0.001)
Total activity (beam breaks)
F
Male
Main effect: Light vs. dark period at day 3 (p<0.01)
Main effect: PAK1 KO vs. PAK2 mKO at day 3 (p<0.05)
G
Main effect: Day 1 vs. 3 (p<0.001)
Main effect: PAK1 KO vs. d1/2 KO (p<0.05)
Main effect: Muscle-specific PAK2 knockout at day 3 (p<0.05)
Energy intake (kJ)
Day 1
Day 3
H
Female
Main effect: Muscle-specific PAK2 knockout at day 3 (p<0.01)
I
Male
Main effect: Day 1 vs. 3 (p<0.001)
J
Female
Main effect: Control vs. d1/2 KO upon refeeding (p<0.05)
Main effect: Muscle-specific PAK2 knockout - Day 3, dark period (p<0.001)
K
Male
Main effect: Light vs. dark period at day 1 (p<0.001)
Main effect: Muscle-specific PAK2 knockout - Day 3, light and dark period (p<0.05)

Figure S4

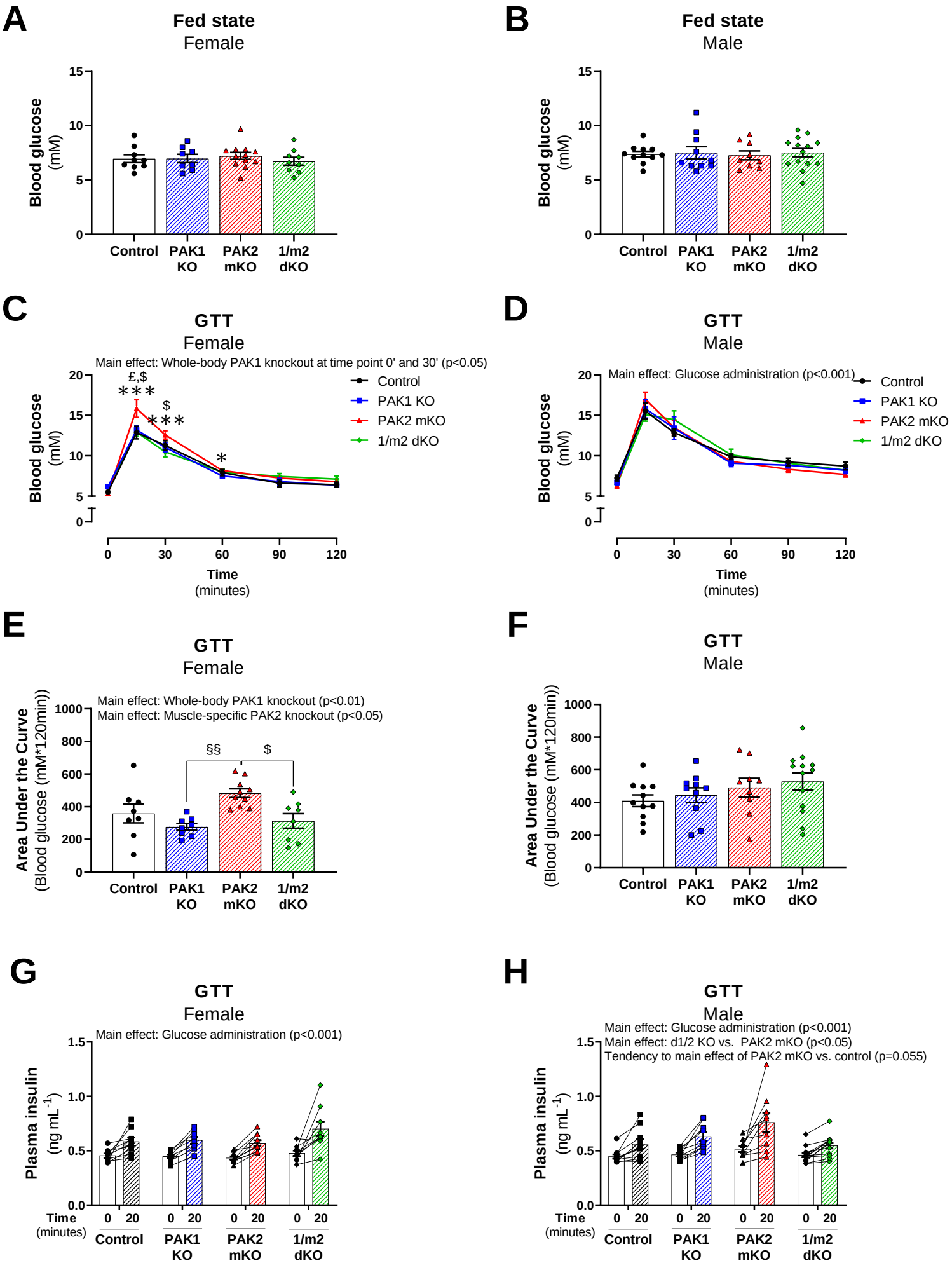
A
Fed state
Female
Blood glucose (mM)
Control
PAK1 KO
PAK2 mKO
1/m2 dKO
B
Fed state
Male
C
GTT
Female
Main effect: Whole-body PAK1 knockout at time point 0' and 30' (p<0.05)
£,$
***
$
***
*
Time (minutes)
D
GTT
Male
Main effect: Glucose administration (p<0.001)
E
GTT
Female
Area Under the Curve (Blood glucose (mM*120min))
Main effect: Whole-body PAK1 knockout (p<0.01)
Main effect: Muscle-specific PAK2 knockout (p<0.05)
§§
$
F
GTT
Male
G
GTT
Female
Main effect: Glucose administration (p<0.001)
Plasma insulin (ng mL-1)
H
GTT
Male
Main effect: Glucose administration (p<0.001)
Main effect: d1/2 KO vs. PAK2 mKO (p<0.05)
Tendency to main effect of PAK2 mKO vs. control (p=0.055)

Figure S5

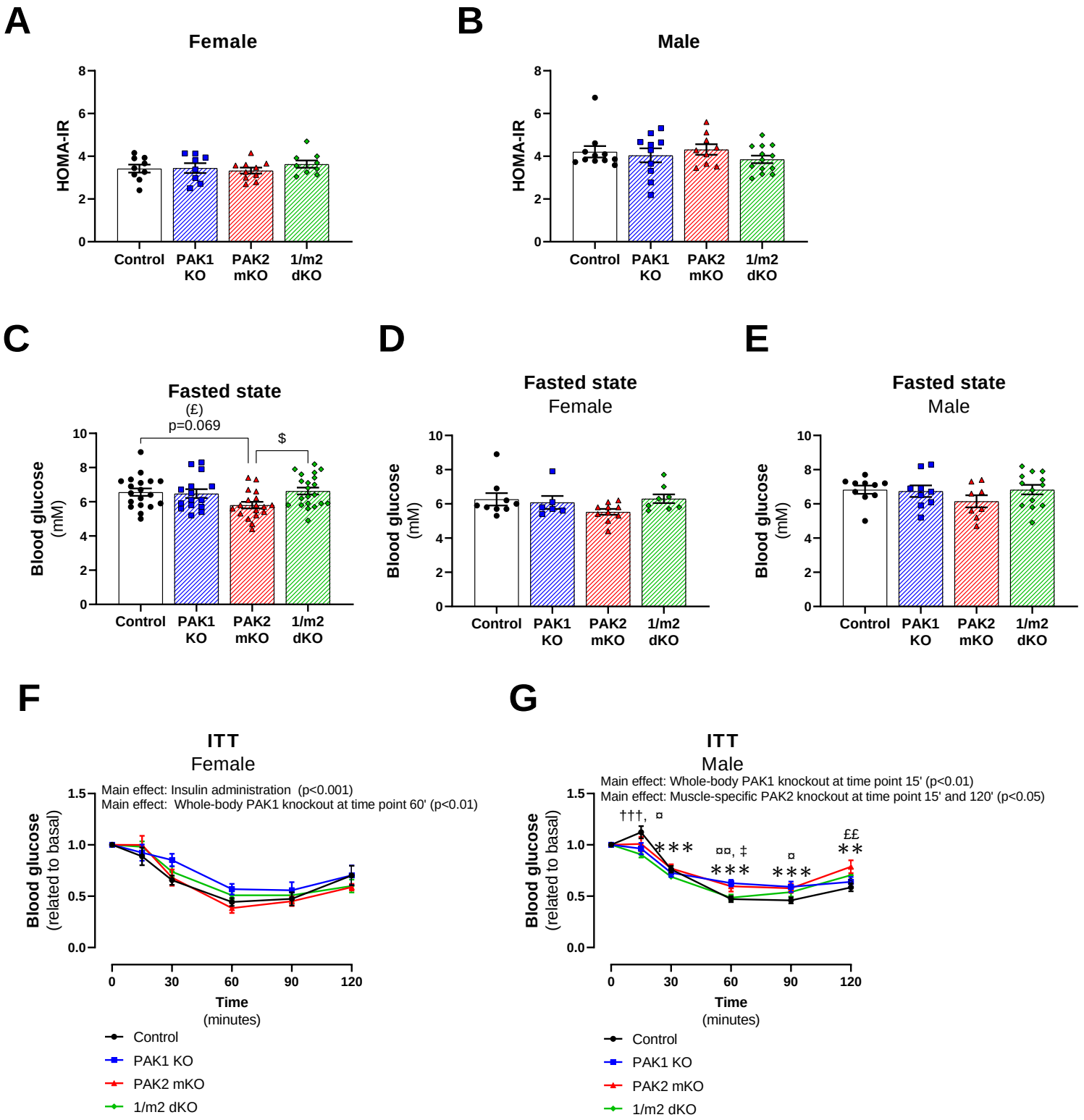
A
Female
HOMA-IR
Control
PAK1 KO
PAK2 mKO
1/m2 dKO
B
Male
C
Fasted state
(£)
p=0.069
$
Blood glucose (mM)
D
Fasted state
Female
E
Fasted state
Male
F
ITT
Female
Main effect: Insulin administration (p<0.001)
Main effect: Whole-body PAK1 knockout at time point 60' (p<0.01)
Blood glucose (related to basal)
Time (minutes)
G
ITT
Male
Main effect: Whole-body PAK1 knockout at time point 15' (p<0.01)
Main effect: Muscle-specific PAK2 knockout at time point 15' and 120' (p<0.05)

Figure S6

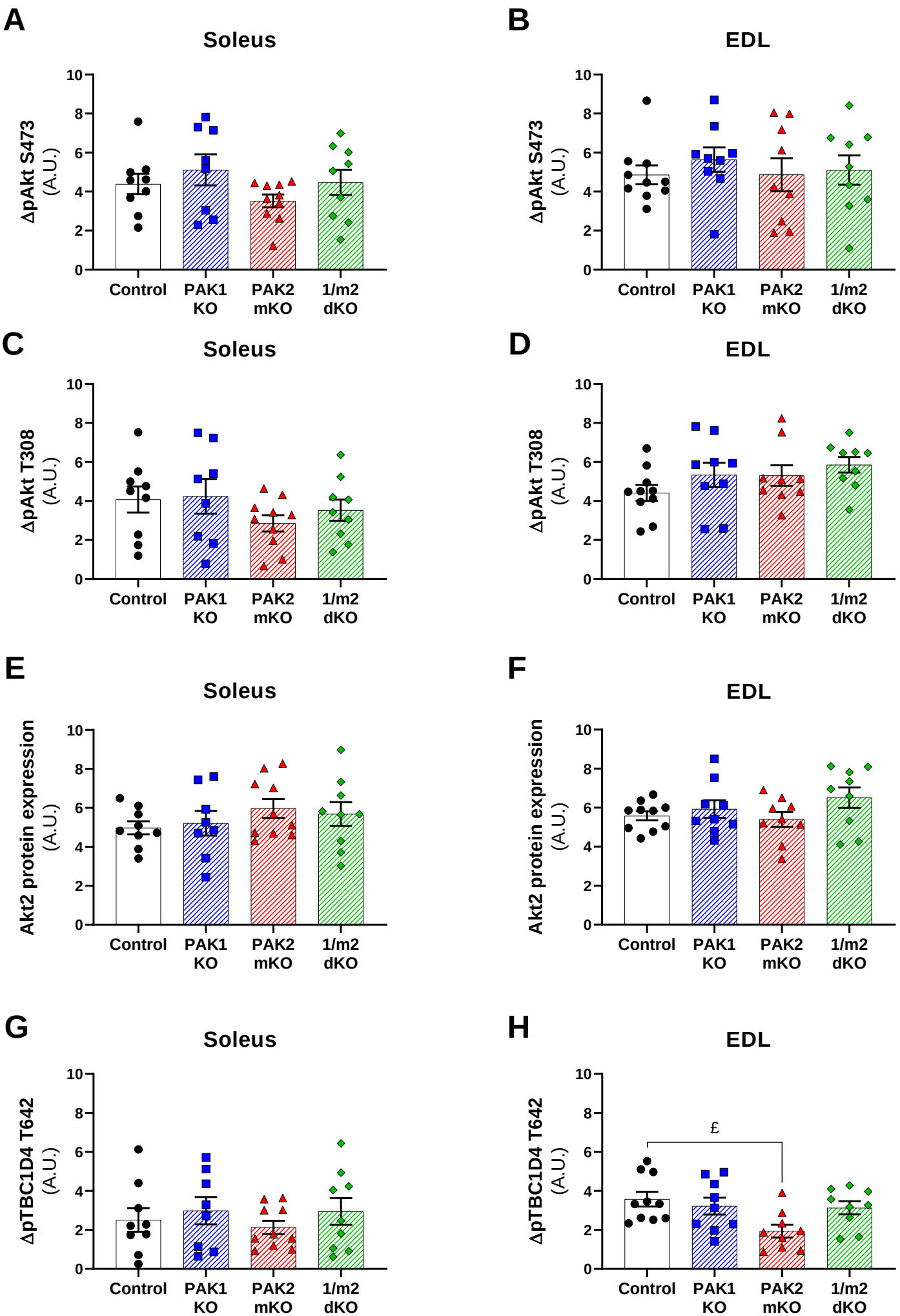

Table 1. Antibody Table

Antibody name	Antibody ID (RRID)	Manufacturer; Catalog Number;	Species Raised in; Monoclonal or Polyclonal	Antibody dilution	Blocking buffer
Akt2	AB_2225186	Cell Signaling Technology; 3063	Rabbit, Monoclonal antibody	1:1000	2% milk
pAkt S473	AB_329825	Cell Signaling Technology; 9271	Rabbit; Polyclonal antibody	1:1000	2% milk
pAkt T308	AB_329828	Cell Signaling Technology; 9275	Rabbit; Polyclonal antibody	1:1000	2% milk
GLUT4	AB_2191454	Thermo Fisher Scientific; PA1-1065	Rabbit; Polyclonal antibody	1:1000	2% milk
PAK1	AB_330222	Cell Signaling Technology; 2602	Rabbit; Polyclonal antibody	1:1000	2% milk
PAK2	AB_2283388	Cell Signaling Technology; 2608	Rabbit; Polyclonal antibody	1:1000	2% milk
pPAK1/2 T423/402	AB_330220	Cell Signaling Technology; 2601	Rabbit; Polyclonal antibody	1:1000	5% BSA
TBC1D4	AB_492639	Millipore; 07-741	Rabbit; Polyclonal antibody	1:1000	2% milk
pTBC1D4 T642	AB_2651042	Cell Signaling Technology; 8881	Rabbit; Monoclonal antibody	1:1000	2% milk